17. PRELIMINARY ORGANIC ANALYSES OF DSDP CORES, LEG 14, ATLANTIC OCEAN[1]

Bernd R. Simoneit, E. Sloan Scott, and A. L. Burlingame, Space Sciences Laboratory, University of California, Berkeley

ABSTRACT

Organic carbon-rich samples from Sites 138 and 144 of DSDP Leg 14 were analyzed. A sample of Oligocene age yielded mainly alkanes, C_nH_{2n+2} for $n = 19$ to 36 with an odd over even predominance; carboxylic acid methyl esters (formed by clay catalysis with solvent methanol), $C_nH_{2n}O_2$ for $n = 14$ to 25 with an even over odd predominance; and steranes (e.g. cholestane, ergostane, and stigmastane), sterones, and triterpanes. The other samples, all of Cretaceous age, yielded mainly alkanes, C_nH_{2n+2} for $n = 19$ to 30^+ with no significant predominance; carboxylic acid methyl esters, $C_nH_{2n}O_2$ for $n = 14$ to 24 with no predominance; and sterones and steranes probably of marine origin. These Cretaceous sediments contain large amounts of kerogen and the extractable petroliferous material appears to have gone through maturation processes.

INTRODUCTION

Organic carbon-rich samples from two drill sites of Leg 14 were analyzed. Site 138 (25°55.4'N, 25°33.8'W) was cored in the abyssal hills (water depth 5288 m) at the foot of the continental rise, about 870 km west of Cap Blanc, West Africa (Hayes et al., 1971). The upper sample is of Oligocene age (approximately 35 m.y.) and consists of dark olive gray clay. The lower sample is of close to middle Cretaceous age (approximately 90-100 m.y.) and consists of a mixture of clay, dolomite, silt, and carbonaceous black clayey mud, all occurring just above an altered aphanitic basalt layer (Pimm, personal communication). Site 144 (9°27.2'N, 54°20.5'W) was cored on the northern flank of the Demerara Rise (water depth 2957 m) approximately 400 km north of Surinam (Hayes et al., 1971). Four organic carbon-rich samples, all of upper Cretaceous age (range approximately 80-93 m.y.), were analyzed from this core. The samples from 181.0 and 190.1 meters below the seabed consist of black zeolitic, calcareous clays and fine laminated black shale. Large quantities of hydrogen sulfide were encountered at this level and the sequence was interbedded with marly limestone (Pimm, personal communication). The samples from 214.7 and 216.1 meters below the seabed consist of laminated dark olive gray calcareous clay with significant amounts of organic particulate matter and fossil foraminifera and nannoplankton. Again large quantities of hydrogen sulfide were encountered at this level. Similar organic-rich laminated sediments from the Black Sea and the Mediterranean Sea have been analyzed (Simoneit, in press; Simoneit et al., in press), and Site 105 in the western Atlantic Ocean also yielded some organic-rich clay sediments (Simoneit et al., 1972).

---

[1]Manuscript received too late to be included in Volume 14.

EXPERIMENTAL PROCEDURES

High resolution mass spectrometric analyses of the benzene/methanol- or tolune/methanol-soluble extracts were carried out on a GEC-AEI MS-902 mass spectrometer on-line to an XDS Sigma 7 computer (described by Burlingame, 1968 and 1970, and Burlingame et al., 1970). The samples were introduced via a ceramic direct inlet probe into the ion source, operated at the following conditions: resolution 10,000; ionizing current 500μA; ionizing voltage 50 eV; and temperature 200 to 220°C. The scan rate was 16 sec per decade with a clock rate of 24 kHz. Multiple scans were taken during each analysis and then sum averaged together during data reduction. Selected high resolution mass spectral data are presented as heteroatomic plots (Burlingame and Smith, 1968) in various figures in the text.

Analyses using gas chromatography-mass spectrometry were carried out on a modified Varian MAT Model 311 GC/MS linked on-line to an XDS Sigma 2 computer (Smith et al., 1971). The GC conditions used in the GC/MS analyses are the same as cited in the respective GC conditions used in the GC/MS analyses are the same as cited in the respective GC figure legends, and the mass spectrometric and computer operating parameters are as reported (Smith et al., 1971). Certain mass spectra from the various GC/MS analyses were identified by use of a compound classifier (Smith, 1972; Chang et al., in preparation).

Gas chromatographic analyses were carried out using a Perkin-Elmer Model 900 gas chromatograph fitted with a flame ionization detector and operating under the conditions stated in the respective figure legends.

All solvents used, e.g., toluene, benzene, methanol, and n-heptane were Mallinckrodt Nanograde quality. The toluene, benzene, and methanol were redistilled in an all glass apparatus prior to use.

All the samples were dried under vacuum (60°C and 25 cm Hg pressure) and then powdered using a mortar and pestle. The dry weights averaged 3 g. The powders were then extracted in a small, all glass Soxhlet apparatus for 3 to 5 days. After filtration through a fine glass frit the extracts were concentrated on a rotary evaporator (bath at 30-40°C) and then repartitioned into a heptane-diethyl ether-soluble fraction and a tolune/methanol- or benzene/methanol-soluble fraction. These fractions were not separated further and were subjected directly to GC and mass spectrometric analyses.

RESULTS

The solvent extract yields from the core samples are listed in Table 1 and the elemental analyses of these samples are found in Table 2.

Site 138

The two Site 138 samples were subjected to GC, HRMS, and GC/MS analyses. The GC traces for the 117.6 meters sample (14-138-2-6) are shown in Figure 1 and the high resolution mass spectrometric data for the toluene/methanol-soluble fraction is shown in Figure 2.[2] The major constituents are hydrocarbons of the series C_nH_{2n+2} to C_nH_{2n-12}, ranging from $n = 3$ to 20; however, not every homolog has been detected. The peaks of compositions $C_{14}H_{23}$ at m/e 191 (Structure I) and $C_{16}H_{25}$ at m/e 217 (Structure II) are significantly above the background. Contaminants from the core tube (dibutyl esters) or phthalate esters are minor. Carboxylic acids or their esters and other oxygenated higher molecular weight compounds have not been detected.

I $C_{14}H_{23}$, m/e 191
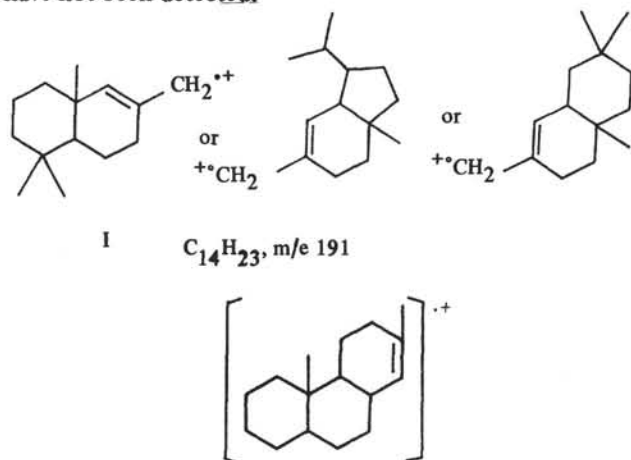
The GC/MS data for the heptane/ether-soluble fraction are summarized in Table 3 and the salient features of these data appear in Figure 3. The major constituents are alkanes, C_nH_{2n+2}, ranging from $n = 18$ to 34 with strong odd over even predominance. Methyl esters of carboxylic acids were detected for the series $C_nH_{2n}O_2$ ranging from $n = 14$ to 25, with an even over odd predominance. Minor amounts of steranes, sterones, and triterpenes were detected. The major components match well to the standard spectra and consist of cholestane (Structure III), ergostane (Structure IV), and sitostane or stigmastane (Structure V). The sterones belong to the series $C_nH_{2n-8}O$ for $n = 27$ to 30. The mass spectrum (scan 270) in Figure 3g fits the fragmentation

III $C_{27}H_{48}$, m/e 371   IV $C_{28}H_{50}$, m/e 386

V $C_{29}H_{52}$, m/e 400
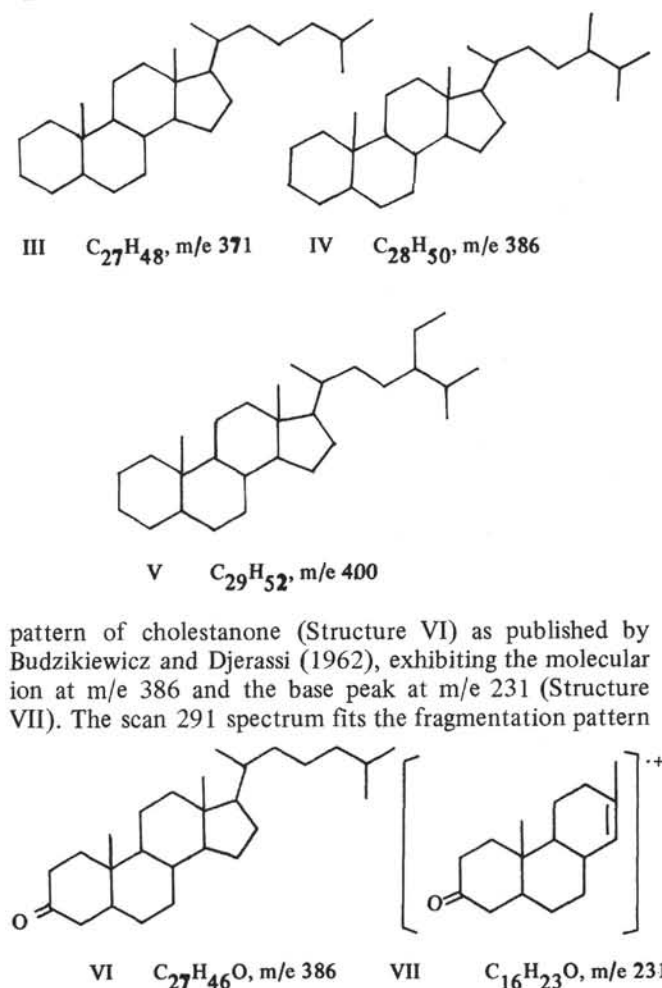
pattern of cholestanone (Structure VI) as published by Budzikiewicz and Djerassi (1962), exhibiting the molecular ion at m/e 386 and the base peak at m/e 231 (Structure VII). The scan 291 spectrum fits the fragmentation pattern

VI $C_{27}H_{46}O$, m/e 386   VII $C_{16}H_{23}O$, m/e 231

---

[2] In this report, all high resolution mass spectra are presented as heteroatomic plots (Burlingame and Smith, 1968) with the masses plotted in methylene units. On the abscissa, each principal division marker corresponds to the saturated alkyl fragment (even-electron ion), for example, C_nH_{2n+1}, with the number of carbon and hydrogen atoms given subsequently. Each principal division of the abscissa is further divided into seven units. The number of hydrogen atoms of an unsaturated or cyclic-fragment ion is obtained by subtracting the number of units (two hydrogen atoms) or half-units from the $2n+1$ hydrogen atoms of the respective saturated principal division, C_nH_{2n+1}. Fragments with more than seven degrees of unsaturation are plotted with each principal division marker on the

abscissa corresponding to the fragment ion C_nH_{2n-13}. Each principal division is again further divided into seven units, and the number of hydrogen atoms of a fragment ion is derived as discussed above. The origin of the abscissas is the same m/e ratio for each plot, thus the nominal masses, indicated in 50 mass unit intervals below the carbon/hydrogen ratio scale, lie directly above one another from plot to plot. All plots are normalized to a base peak (usually the base peak of the entire spectrum, unless otherwise specified) on the relative intensity scale. In order to make high mass, low intensity features of the spectrum observable, the whole spectrum or any region thereof can be multiplied by a scale factor. This factor is indicated by /X00 at the point of scale expansion. A composite low resolution mass spectrum for each set of data appears plotted separately at the bottom of the plot series.

TABLE 1
DSDP Small Core Sample Extracts, Leg 14

Sample	Depth Below Seafloor (m)	Approximate Age	Organic Carbon %[a]	Heptane/Ether Extract %	Benzene/Methanol Extract %
14-138-2-6 (12-13 cm)	117.6	Oligocene	2.3	0.15	0.42
14-138-6-3 (49-50 cm)	428.5	Middle Cretaceous	16.8	0.44	1.22
14-144A-5-1 (114-116 cm)	181.0	Upper Cretaceous	11.1	0.04	0.14
14-144A-6-1 (100-101 cm)	190.1	Upper Cretaceous	10.4	0.35	0.92
14-144-4-2 (20-21 cm)	214.7	Upper Cretaceous	10.3	0.27	0.70
14-144-4-3 (14-15 cm)	216.1	Upper Cretaceous	6.5	0.23	1.03

[a]Data supplied by G. Bode, DSDP staff.

TABLE 2
Elemental Analyses of DSDP Core Samples From Leg 14

Sample		Total C (%)	H (%)	Residue (%)	Oxygen (%)[a]
14-138-2-6 (12-13 cm)	dried	2.59	1.56	84.9	10.9
	extracted	2.47	1.42	86.9	9.2
14-138-6-3 (49-50 cm)	dried	11.99	1.91	76.6	9.5
	extracted	11.21	1.79	77.9	9.1
14-144A-5-1 (114-116 cm)	dried	11.26	0.31	62.5	25.9
	extracted	12.72	0.34	59.4	27.5
14-144A-6-1 (100-101 cm)	dried	16.45	1.59	62.0	20.0
	extracted	15.54	1.50	63.3	20.7
14-144-4-2 (20-21 cm)	dried	13.37	1.85	74.0	10.8
14-144-4-3 (14-15 cm)	dried	15.04	1.21	61.5	22.2
	extracted	13.52	1.14	62.1	23.2

[a]Determined by difference.

of ergostanone (Structure VIII) and the scan 322 spectrum (cf. Figure 3h) fits for stigmastanone (Structure IX). The triterpanes belong to the series C_nH_{2n-8} and C_nH_{2n-10} for $n = 30$ to 31. The major peak in these data is due to dibutyl

VIII $C_{28}H_{48}O$, m/e 400


IX $C_{29}H_{50}O$, m/e 414
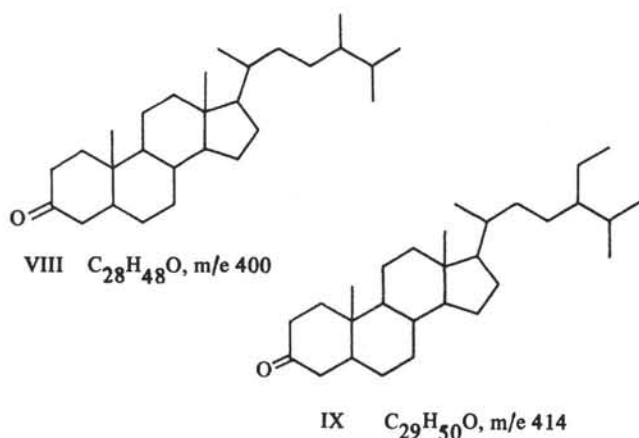
azelate, probably from core tube contamination. Phthalate esters were detected as minor components and probably derive from the sample vial caps.

The scan 191 mass spectrum (cf. Figure 3f) occurs at the maximum concentration of an unknown compound of molecular weight 382, which exhibits a base peak of m/e 115 (cf. Figure 3e). The fragmentation pattern appears to fit a diester of glutaric acid, probably octyl (5-cyclopentylpentyl) glutarate, and this compound is a possible contaminant from the core tube material.

The GC traces for the 428.5 meter sample (14-138-6-3) are shown in Figure 4 and the GC/MS data are also summarized in Table 3. The salient features of the GC/MS data are shown in Figure 5. The alkanes, C_nH_{2n+2}, are again the major constituents of the heltane/ether fraction and range from $n = 13$ to 26 with no predominance and maximizing at $n = 17$. Significant amounts of carboxylic acid methyl esters are also present; the series $C_nH_{2n}O_2$ extends from $n = 9$ to 24 with no predominance apparent and maximum at $n = 16$. Sterones and minor amounts of steranes and triterpanes were detected. The steranes were in the series C_nH_{2n-6} for $n = 27$ to 28; the sterones, $C_nH_{2n-8}O$, ranged from $n = 27$ to 29 (the spectrum of cholestanone and stigmastanone appear in Figure 5g and h respectively); and the triterpanes, $C_nH_{2n-(8 \text{ to } 12)}$, were found for $n = 30$ to 31. The scan 106 spectrum (Figure 5f) is an unknown compound of molecular weight 250. Pristane and to a much lesser extent phytane were detected in this sample. Contaminants from the core tube material were also identified, as well as trace amounts of phthalates from the sample vial caps.

Site 144

The four Site 144 samples were subjected to GC, GC/MS, and HRMS analyses. The GC traces for the 181.0 meter sample (14-144A-5-1) are shown in Figure 6. The GC/MS data of the heptane/ether-soluble fraction are summarized in Table 4 and the salient features are shown in Figure 7. Methyl esters of carboxylic acids are present in

577
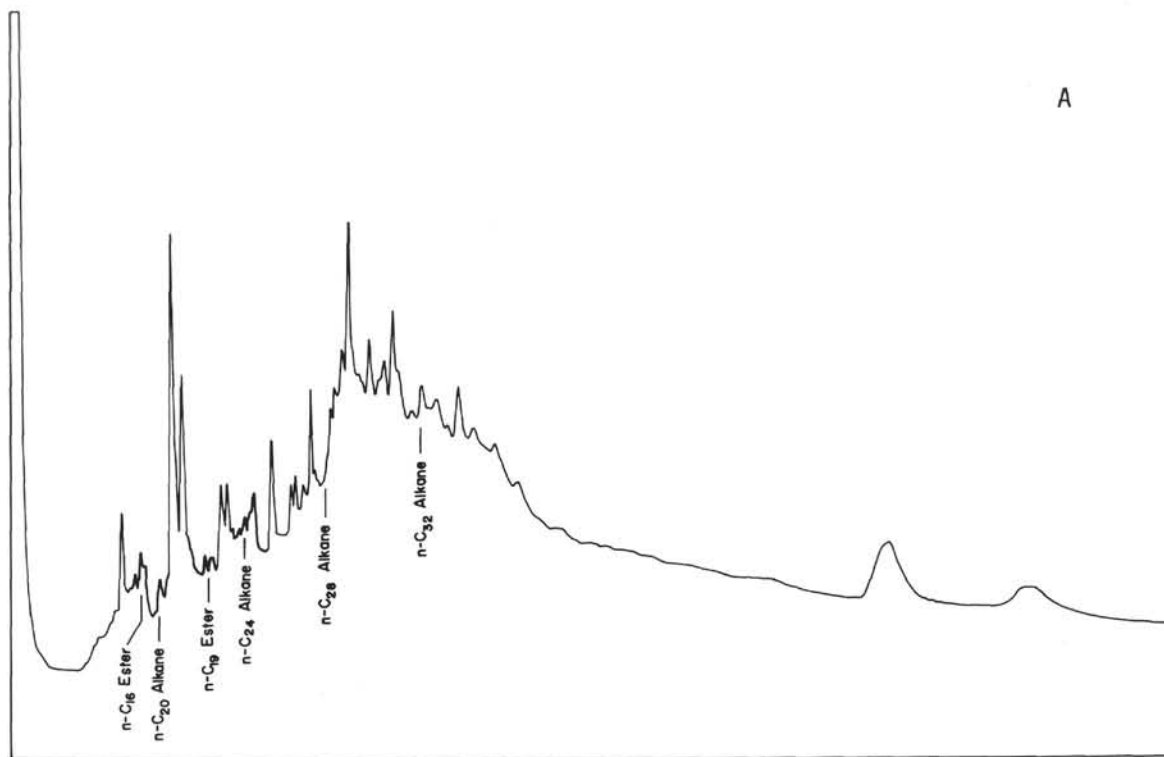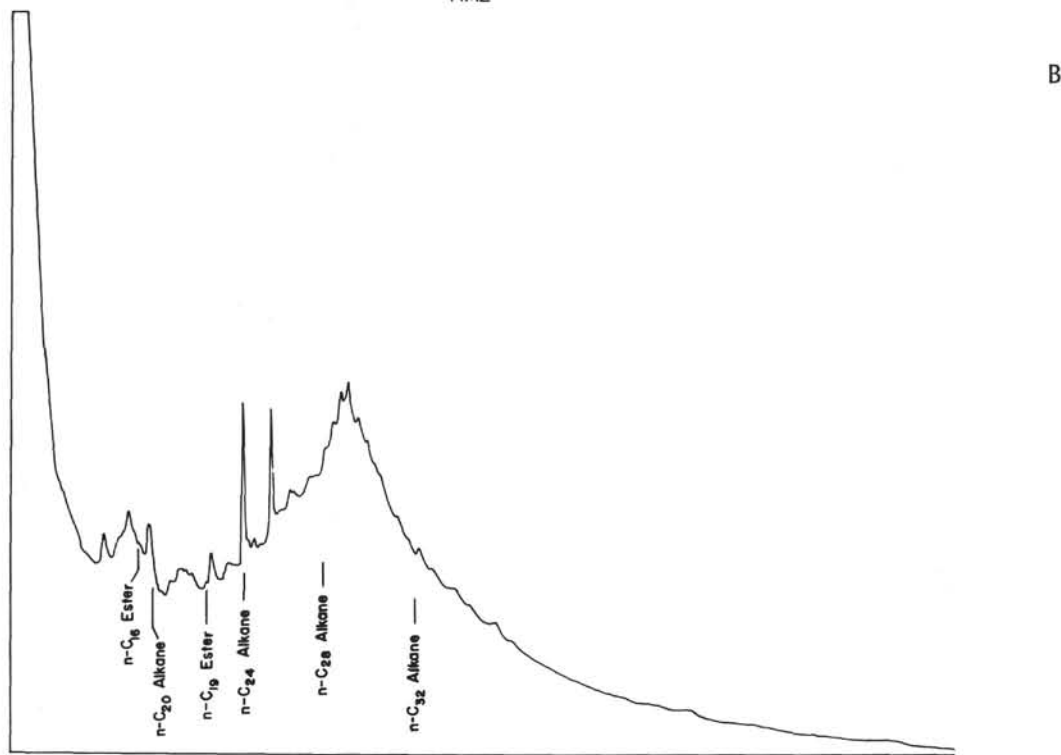
Figure 1a. *Gas chromatogram of the heptane/ether-soluble extract fraction from Sample 14-138-2-6 (12-13 cm). (Conditions: 7.5 ft × 1/8 in. stainless steel column packed with 3% OV-1 on 100-200 mesh gas chrom Q, programmed from 100-275°C at 8°/min and using He carrier gas at 60 ml/min). The relative retention times of various normal alkanes and methyl esters of normal carboxylic acids are indicated on the GC traces (determined by coinjection).*

Figure 1b. *Gas chromatogram of the toluene/methanol-soluble extract fraction from Sample 14-138-2-6 (12-13 cm). (Conditions as cited in Figure 1a).*
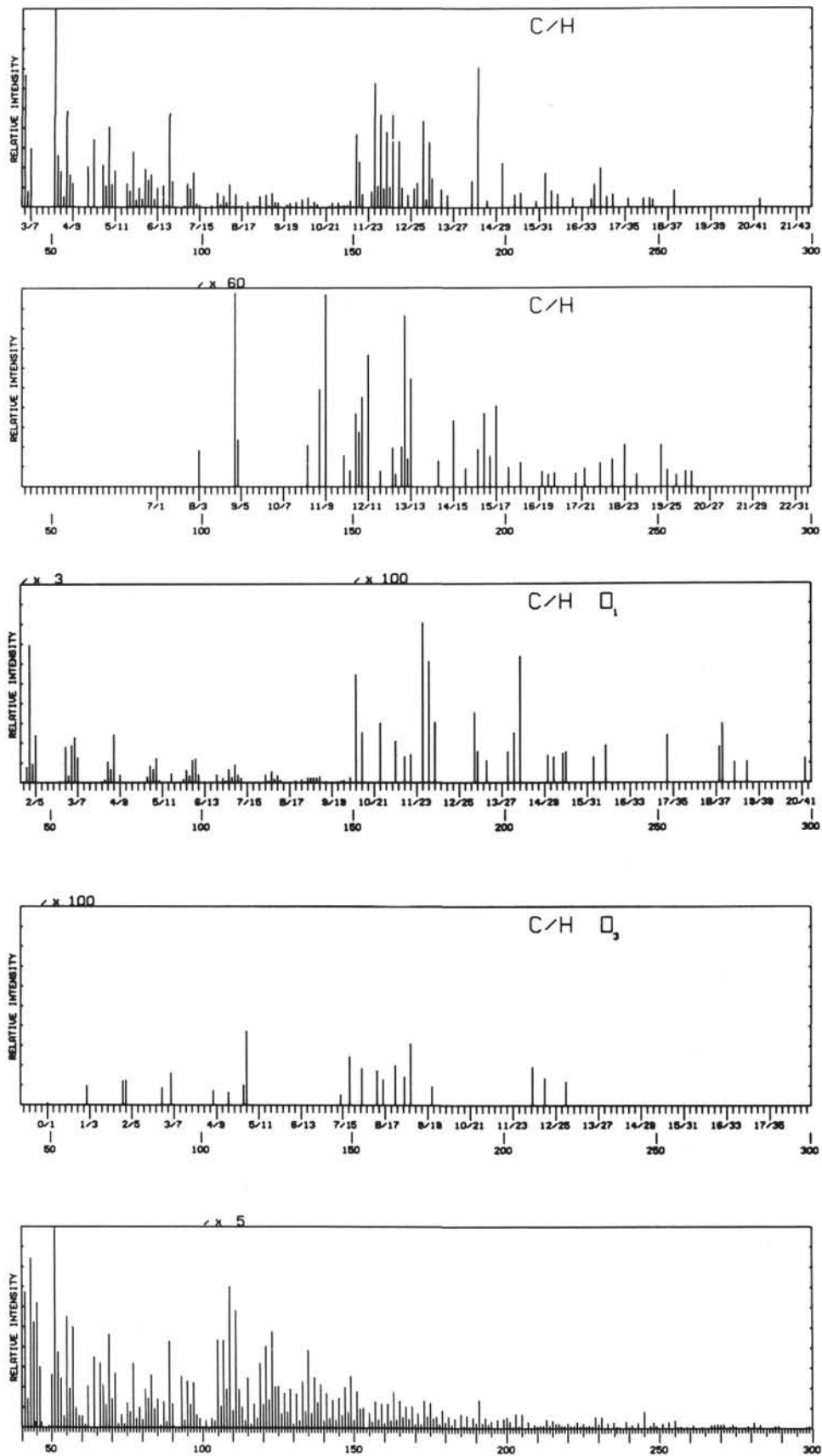
Figure 2. *Partial high resolution mass spectrometric data for the toluene- and methanol-soluble fraction from the exhaustive extract of Sample 14-138-2-6 (12-13 cm).*

TABLE 3
Major Components of the Heptane/Ether-Soluble Extracts from the Core Samples
of DSDP Site 138, Determined by GC/MS

Compound Name	Composition and Molecular Weight		14-138-2-6 (12-13 cm) Spectrum Scan No. (cf. Fig. 3a)	14-138-6-3 (49-50 cm) Spectrum Scan No. (cf. Fig. 5a)
Methyl n-nonanoate	$C_{10}H_{20}O_2$	172	n.d.	5
Methyl caprate	$C_{11}H_{22}O_2$	186	n.d.	17
Acenaphthene	$C_{12}H_{10}$	154	n.d.	27
n-Tetradecane	$C_{14}H_{30}$	198	n.d.	30
Methyl n-undecanoate	$C_{12}H_{24}O_2$	200	n.d.	33
n-Pentadecane	$C_{15}H_{32}$	212	n.d.	48
Methyl laurate	$C_{13}H_{26}O_2$	214	n.d.	52
Diethyl phthalate[b]	$C_{12}H_{14}O_4$	222	n.d.	65
n-Hexadecane	$C_{16}H_{34}$	226	n.d.	71
Methyl n-tridecanoate	$C_{14}H_{28}O_2$	228	n.d.	73
n-Heptadecane	$C_{17}H_{36}$	240	n.d.	89
Pristane	$C_{19}H_{40}$	268	n.d.	90
Methyl myristate	$C_{15}H_{30}O_2$	242	94	91
n-Octadecane	$C_{18}H_{38}$	254	114	102
Phytane	$C_{20}H_{42}$	282	n.d.	103
Methyl n-pentadecanoate	$C_{16}H_{32}O_2$	256	116	104
Unknown	–	250	120	106
n-Nonadecane	$C_{19}H_{40}$	268	137	113
Methyl palmitate	$C_{17}H_{34}O_2$	270	140	115
Dibutyl phthalate[b]	$C_{16}H_{22}O_4$	278	142	n.d.
n-Eicosane	$C_{20}H_{42}$	282	156	123
Methyl margarate	$C_{18}H_{36}O_2$	284	158	125
Dibutyl azelate	$C_{17}H_{32}O_4$	300	163	125
Methyl stearate	$C_{19}H_{38}O_2$	298	170	136
n-Heneicosane	$C_{21}H_{44}$	296	171	n.d.
Dibutyl sebacate[a]	$C_{18}H_{34}O_4$	314	173	138
n-Docosane	$C_{22}H_{46}$	310	178	n.d.
Methyl n-nonadecanoate	$C_{20}H_{40}O_2$	312	180	146
n-Tricosane	$C_{23}H_{48}$	324	186	n.d.
Methyl arachidate	$C_{21}H_{42}O_2$	326	187	155
Unknown	–	382	191	n.d.
n-Tetracosane	$C_{24}H_{50}$	338	195	n.d.
Methyl n-heneicosanoate	$C_{22}H_{44}O_2$	340	196	164
n-Pentacosane	$C_{25}H_{52}$	352	204	n.d.
Methyl behenate	$C_{23}H_{46}O_2$	354	205	175
Dioctyl phthalate[b]	$C_{24}H_{38}O_4$	390	206	n.d.
n-Hexacosane	$C_{26}H_{54}$	366	215	n.d.
Methyl tricosanoate	$C_{24}H_{48}O_2$	368	217	185
n-Heptacosane	$C_{27}H_{56}$	380	229	n.d.
Methyl lignocerate	$C_{25}H_{50}O_2$	382	231	195
Cholestane	$C_{27}H_{48}$	372	241	221
n-Octacosane	$C_{28}H_{58}$	394	244	n.d.

TABLE 3 – *Continued*

| | | | Sample | |
| | | | 14-138-2-6 (12-13 cm) | 14-138-6-3 (49-50 cm) |
Compound Name	Composition and Molecular Weight		Spectrum Scan No. (cf. Fig. 3a)	Spectrum Scan No. (cf. Fig. 5a)
Methyl pentacosanoate	$C_{26}H_{52}O_2$	396	248	n.d.
Ergostane	$C_{28}H_{50}$	386	262	236
n-Nonacosane	$C_{29}H_{60}$	408	263	n.d.
Methyl cerotate	$C_{27}H_{54}O_2$	410	268	n.d.
Triterpane	$C_{30}H_{48}$	408	269	284
Cholestanone	$C_{27}H_{46}O$	386	270	291
Sterane	$C_{29}H_{50}$	398	272	n.d.
Stigmastane (sitostane)	$C_{29}H_{52}$	400	272	282
n-Triacontane	$C_{30}H_{62}$	422	288	n.d.
Sterone	$C_{28}H_{48}O$	400	291	332
Sterane	$C_{30}H_{54}$	414	294	n.d.
n-Hentriacontane	$C_{31}H_{64}$	436	315	n.d.
Triterpane	$C_{30}H_{50}$	410	316	332
Triterpane	$C_{30}H_{52}$	412	316	332
Methyl octacosanoate	$C_{29}H_{58}O_2$	438	321	n.d.
Stigmastanone	$C_{29}H_{50}O$	414	322	364
Dotriacontane	$C_{32}H_{66}$	450	346	n.d.
Sterone	$C_{30}H_{52}O$	428	352	n.d.
n-Tritriacontane	$C_{33}H_{68}$	464	384	n.d.
Triterpane	$C_{31}H_{54}$	426	385	386
Tetratriacontane	$C_{34}H_{70}$	478	419	n.d.

[a]   Probably core tube contamination.
[b]   Probably bagging contamination.
n.d. – Not detected.

almost equal abundance; the series $C_nH_{2n}O_2$ ranges from $n = 14$ to 22, also with no specific predominance and a bimodal maximum at $n = 16$ and 18 (cf. Figure 7c). Small amounts of steranes and triterpanes were detected. The steranes found are in the series C_nH_{2n-6} ranging from $n = 27$ to 29 and two triterpanes, $C_{30}H_{48}$ and $C_{30}H_{54}O$, were detected. The major sterane components match the fragmentation patterns of cholestane (Structure III), ergostane (Structure IV), and sitostane (Structure V) respectively. Each of the spectra exhibiting the triterpane compositions (i.e., molecular ions, M - CH_3, and large m/e 191 peaks) is a mixture of several compounds. Minor amounts of phthalate ester contaminants were detected. An unknown compound of molecular weight 476, possible composition $C_{34}H_{68}$, and the less saturated homolog at m/e 474, were detected. These compounds have a base peak at m/e 213 (cf. Figure 7d).

The GC traces for the 190.1 meter sample (14-144A-6-1) are shown in Figure 8. The GC/MS data of the heptane/ether-soluble fraction are summarized in Table 4 and the salient features are shown in Figure 9. There were two major component series present in this case. The carboxylic acids (detected as the methyl esters) of the series $C_nH_{2n}O_2$ ranged from $n = 14$ to 24, with no predominance and a maximum at $n = 16$ (cf. Figure 9c). An unknown group of compounds exhibiting molecular ions at m/e 490, 488, 476, 474, 460, 446, and 444 were present, with the homolog at m/e 476 (cf. scan 300 in Figure 9h) being the most abundant. These compounds exhibit a base peak at m/e 213 (cf. Figure 9d) and were found in minor amounts at the 181.0 meter level of this core. No known chemical structures could at this time be fit to the mass spectrometric fragmentation pattern of these compounds; however, from the ratio of the ^{13}C isotope parent peak to the parent ion, the compositional series C_nH_{2n} (for $n = 34$ and 35) and C_nH_{2n-2} (for $n = 32$ to 35) appear to fit the data best. The compound of mass 476 (cf. Figure 9h) fragments by losing: CH_3 to m/e 461, C_6H_{13} to m/e 391, and C_8H_{17} to m/e 363, which indicates an isoprenoidal C_8 sidechain.

The alkanes were found in lesser amounts. The series C_nH_{2n+2} ranged from $n = 16$ to 30, with a slight odd over even predominance and maximizing at $n = 17$. There is also a large amount of *iso*-tetradecane in this mixture (cf. scan 45 in Figure 9f). The mass spectrum (cf. scan 159 in Figure
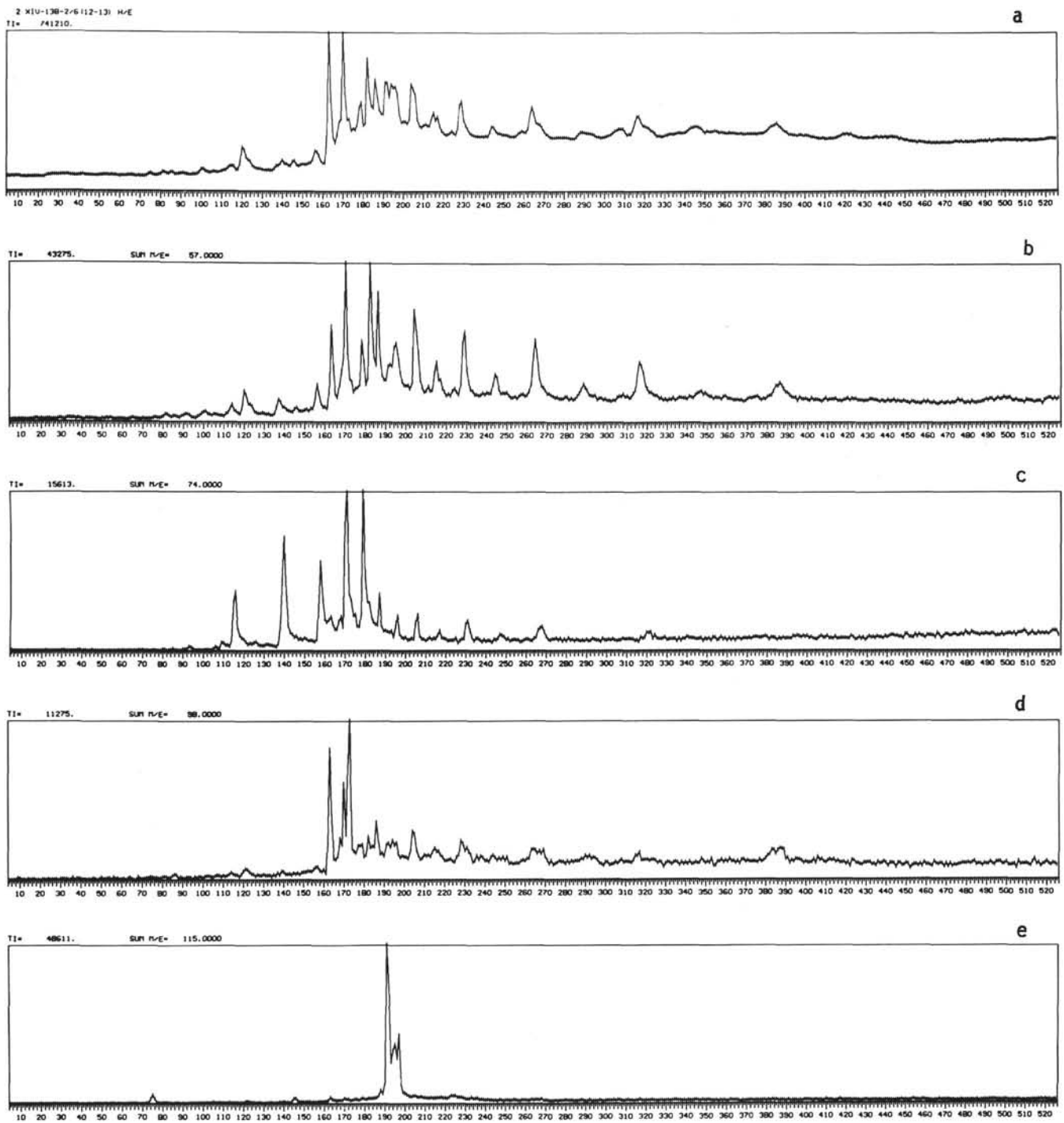
Figure 3. *GC/MS data for total heptane-soluble extract from Sample 14-138-2-6 (12-13 cm). (GC conditions as cited in Figure 1a).*

a) *total ionization sum plot.*
b) *m/e 57 sum plot.*
c) *m/e 74 sum plot.*
d) *m/e 98 sum plot.*
e) *m/e 115 sum plot.*
f) *Mass spectrum scan 191 (unknown, M-382).*
g) *mass spectrum scan 270 (cholestanone).*
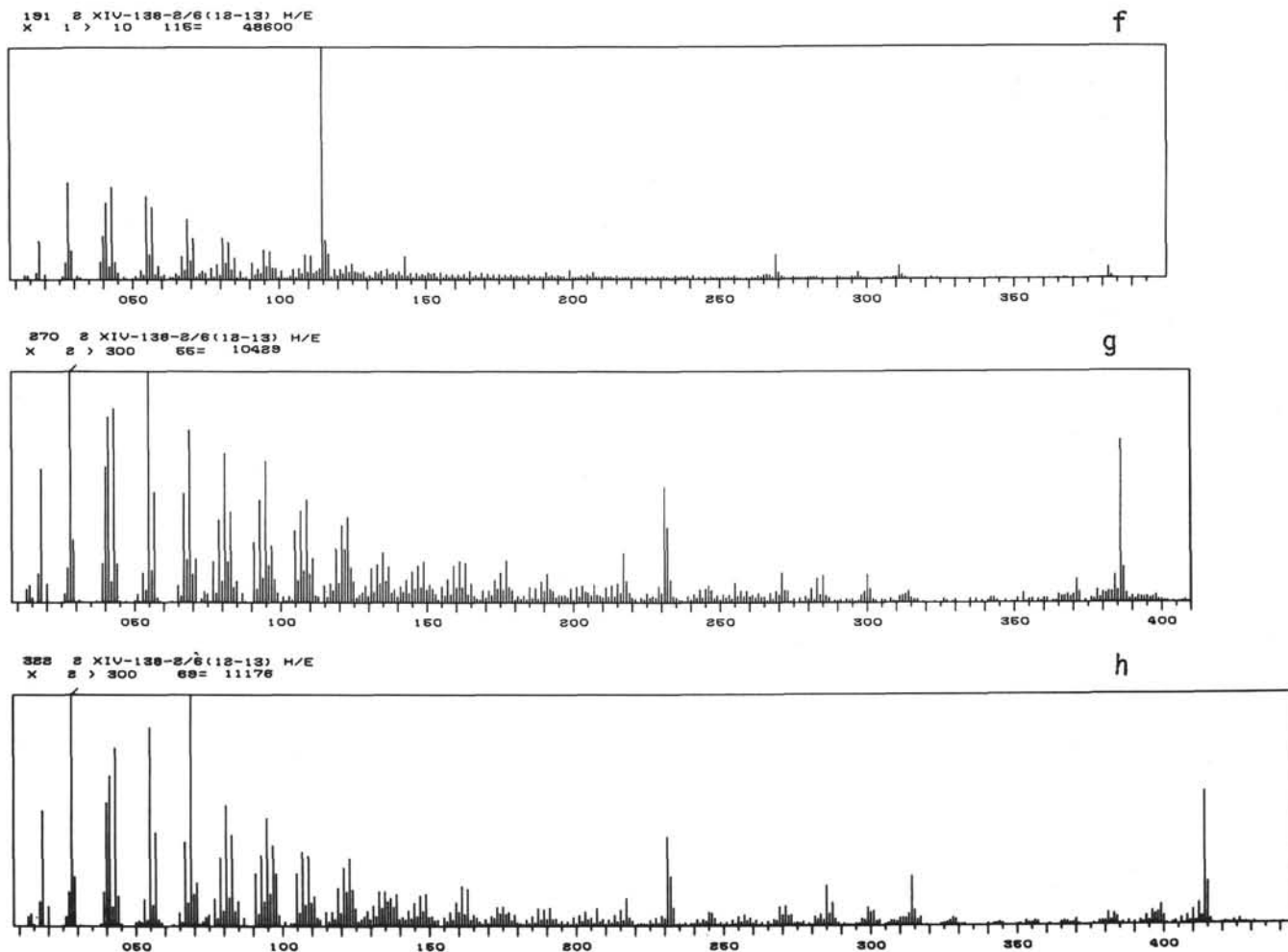h) *mass spectrum scan 322 (stigmastanone).*

Figure 3. *(Continued)*.

9g) of the largest peak in the GC trace (cf. Figure 8a) fits the fragmentation pattern of dibutyl azelate. The homologs $n = 17$ to 19 of this series, $C_nH_{2n-2}O_4$ were detected and are probably derived from core tube contamination. Phthalate ester contaminants were not found.

The GC traces for the 214.7 meter sample (14-144-4-2) are shown in Figure 10 and the high resolution mass spectrometric data of the toluene- and methanol-soluble fraction are shown in Figure 11. A low amount of dibutyl phthalate is present, as indicated by the peaks of compositions $C_8H_5O_3$, $C_8H_7O_4$, $C_{12}H_{15}O_4$, and $C_{16}H_{22}O_4$. Significant amounts of hydrocarbons are present for the series C_nH_{2n+2} to C_nH_{2n-14} for $n = 3$ to 30, however, not every homolog was detected. Minor amounts of sterols or sterones of the series $C_nH_{2n-8}O$ and $C_nH_{2n-10}O$ for $n = 27$ to 29 were also found in this sample. The peaks at m/e 217 of composition $C_{16}H_{25}$ (Structure II) and at m/e 215 of composition $C_{16}H_{23}$ (Structure X) are significantly above the background, corroborating the presence of steroidal compounds. Carboxylic acids or their esters were not detected in these data.

The GC traces of the 216.1 meter sample (14-144-4-3) are shown in Figure 12. The GC/MS data are summarized in Table 4 and the salient features are shown in Figure 13. The
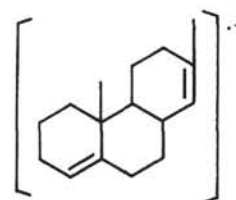
X $C_{16}H_{23}$, m/e 215

GC trace of the heptane/ether-soluble fraction strongly resembles the GC trace of the same fraction of the 214.7 meter sample (14-144 4-2) (cf. Figure 10a). The major components are hydrocarbons of the series C_nH_{2n+2}, ranging from $n = 14$ to 28, with no predominance and a maximum at $n = 17$. Lesser amounts of carboxylic acids (as the methyl esters) and steranes were detected. The acid series, $C_nH_{2n}O_2$, ranged from $n = 11$ to 24, with no predominance and a maximum at $n = 18$ (cf. Figure 13c). The major steroidal compounds found are of the series C_nH_{2n-6}, ranging from $n = 27$ to 30 and the mass spectra fit the fragmentation patterns of cholestane (Structure III)
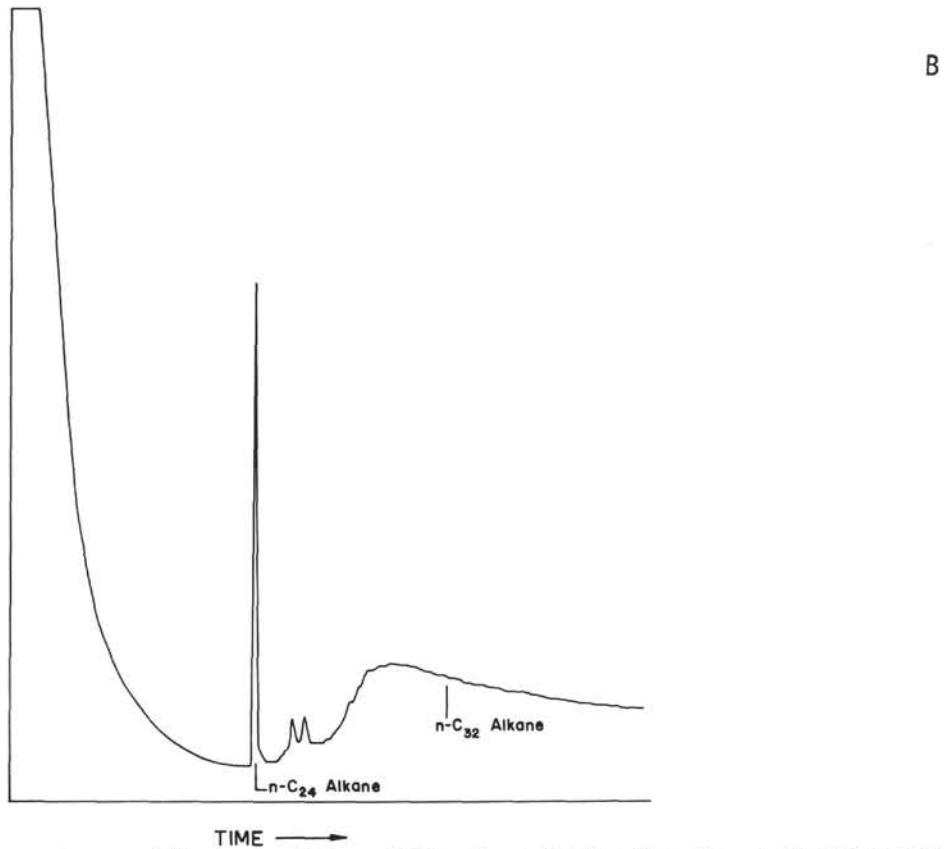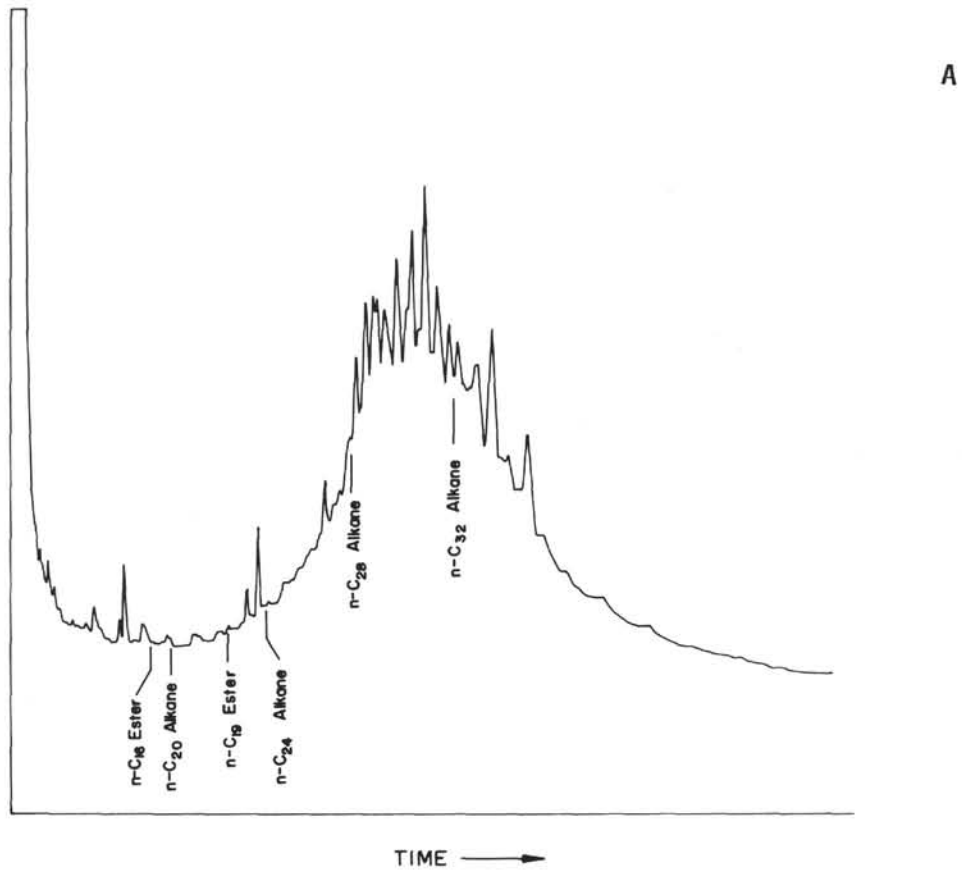
583

Figure 4a. *Gas chromatogram of the heptane/ether-soluble extract fraction from Sample 14-138-6-3 (49-50 cm). Conditions as cited in Figure 1a.*

Figure 4b. *Gas chromatogram of the benzene/methanol-soluble extract fraction from Sample 14-138-6-3 (49-50 cm). Conditions as cited in Figure 1a.*

(cf. scan 320 in Figure 13g), ergostane (Structure IV), and sitostane (Structure V) (cf. scan 349 in Figure 13h) respectively. The scan 141 spectrum (cf. Figure 13f) fits the fragmentation pattern of *iso*-nonadecane, one of the few *iso*-alkanes found in these samples. The unknown compound series (C_nH_{2n} and C_nH_{2n-2}, $n = 32$-35) found in the Samples 14-144A-5-1 and 14-144A-6-1 were not detected and triterpenoidal compounds were also not present. The major GC peak (at lower retention time in Figure 12a) is again dibutyl azelate, probably from core tube contamination. Phthalate esters were detected in minor amounts only.

The benzene- and methanol-soluble extract fractions of the samples from the Leg 14 Sites 138-2-6 (12-13), 138-6-3 (49-50), 144A-5-1 (114-116), 144-4-2 (20-21), and 144-4-3 (14-15) exhibited one dominant GC component (cf. Figures 1b, 4b 6b, 10b and 12b). This peak is found in small quantities in the Core Barrel Extract (Simoneit et al., 1972, Leg 11) and is a major component of the Black Sea core sample 1474 (855 cm level) (Simoneit, in press). A representative GC/MS scan of this compound is shown in Figure 14. From high resolution mass spectrometric data the base peak, m/e 129, has the composition $C_6H_9O_3$ and m/e 147 is $C_6H_{11}O_4$. The compound is dioctyl or di-*iso*-heptyl 2,3-dimethylsuccinate (Structure XI) and its mass spectrometric fragmentation pattern is shown by Structures XI to XV. Synthetic dioctyl
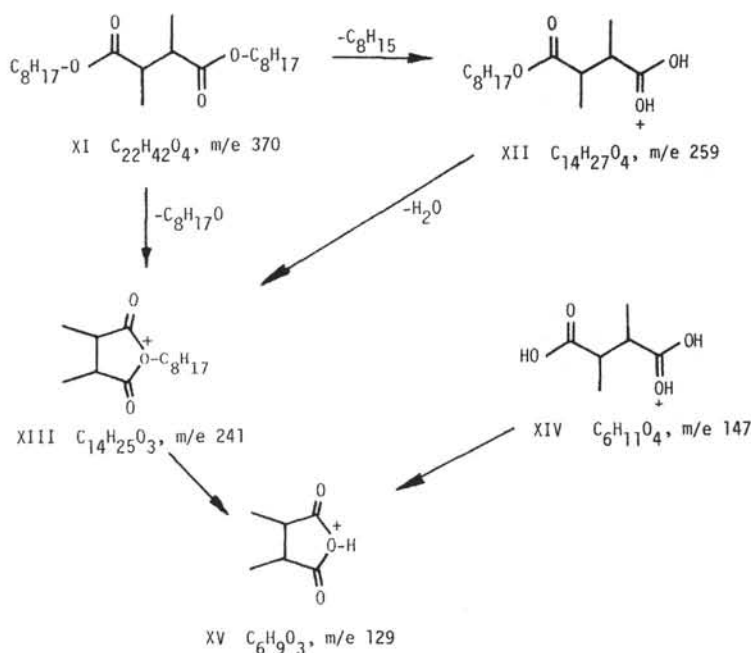
2,3-dimethylsuccinate exhibits an identical mass spectrum and the same GC retention time as this major compound in the benzene and methanol extract fractions.

DISCUSSION AND CONCLUSION

These samples constitute some of the richest (with respect to organic carbon) analyzed to date (Simoneit and Burlingame, 1971a and b, and 1972a and b; Simoneit et al., 1972, in press, and in preparation). The relatively low amounts of solvent-extractable material indicate that the bulk of the organic carbon in these samples is present as kerogen (cf. Table 1). All the extracts contained significant amounts of carboxylic acid esters, which probably formed during the extraction by clay catalyzed esterification of the acids with solvent methanol. Arpino and Ourisson (1971) observed the same phenomenon during extractions of terrestrial sediments. The amounts of acids in these samples thus derivatized indicate that the clay content still has a significant portion of the organic carbon bound as fatty acid salts (adipocere). It has been well established that clay is a good fatty acid scavenger (Simoneit et al., 1972, in press, and in preparation; Meyers and Quinn, 1971).

The distribution histogram for Sample 14-138-2-6 (12-13 cm) of Oligocene age is shown in Figure 15a. The alkanes exhibit a strong odd to even predominance and marine alkanes maximizing at C_{17} are absent. The carboxylic acid distribution maximizes at C_{18} with an even to odd predominance. The soluble organic matter in this sample appears to be derived mainly from terrigenous sources.

The distribution histogram for Sample 14-138-6-3 (49-50 cm) of Cretaceous age is shown in Figure 15b. The alkanes and acids exhibit no homolog predominance and maximize in concentration at C_{17} and C_{16} respectively. Only steranes consisting mainly of cholestane, ergostane, and sitostane, and the corresponding sterones, are present and are probably all of marine derivation. The narrow distribution envelope of both alkanes and acids (cf. Figure 15b) substantiates the pure marine source of this sample's soluble organic matter. The geological history of Site 138 indicates that symmetrical cycles of black cherty muds and dolomitic clayey silts were deposited during the Cretaceous. The origin of these 20 to 30 cm thick sedimentary cycles may possibly indicate a fluctuating chemical environment (Hayes, Pimm et al., 1972). Sample 14-138-6-3 (49-50 cm) was thus probably sedimented during a productive marine plankton bloom.

The distribution histograms of the Site 144 samples, all of Cretaceous age, are shown in Figure 16. Sample 14-144A-5-1 (114-116 cm) exhibits no homolog predominance for the alkanes and acids and they maximize at C_{17} and C_{16} respectively. Again, the narrow distribution envelope of both the alkanes and acids (cf. Figure 16a) indicates essentially a marine source of the soluble organic matter. Sample 14-144A-6-1 (100-101 cm) (cf. Figure 16b) contains a low amount of alkanes, maximizing at C_{17}, with a slight odd to even predominance and extending to C_{30}. The acids exhibit a narrow envelope maximizing at C_{16} and the major components are a series of probably cyclic hydrocarbons maximizing at C_{34} (cf. Figure 16b). The source of this soluble organic matter appears to be marine, and it may have had a major contribution from an unknown species analogous to the present day alga *Botryococcus braunii*, which contains various C_{34} hydrocarbons at one stage of its life cycle (Maxwell et al., 1968).
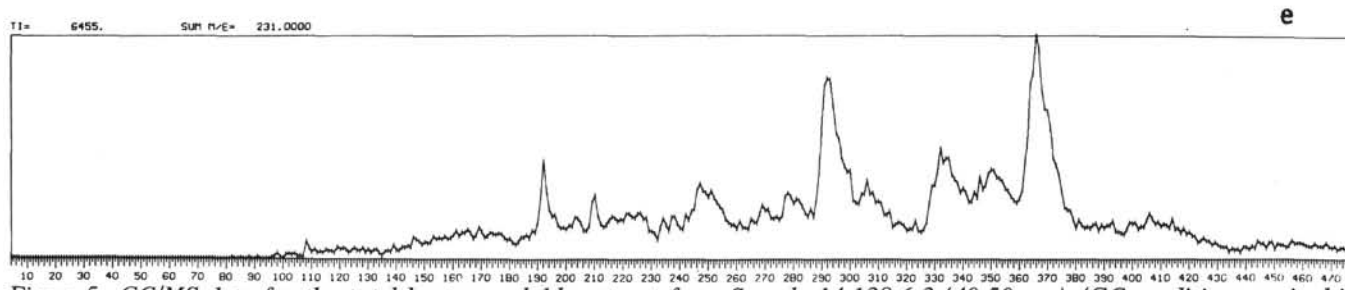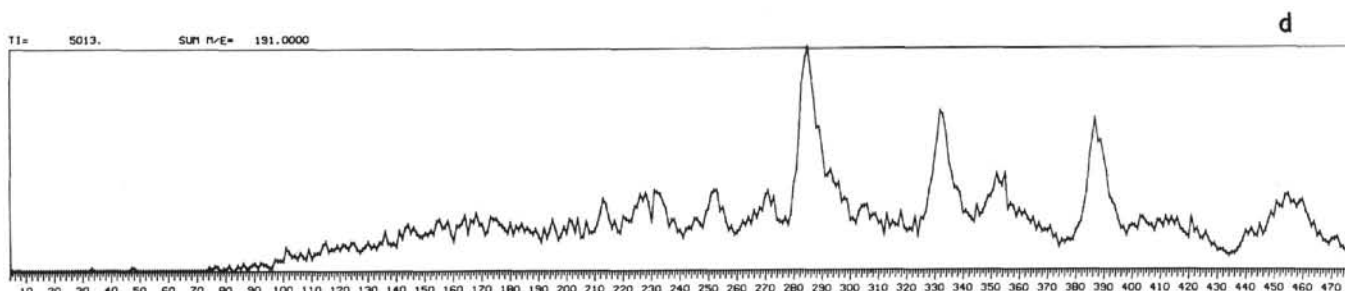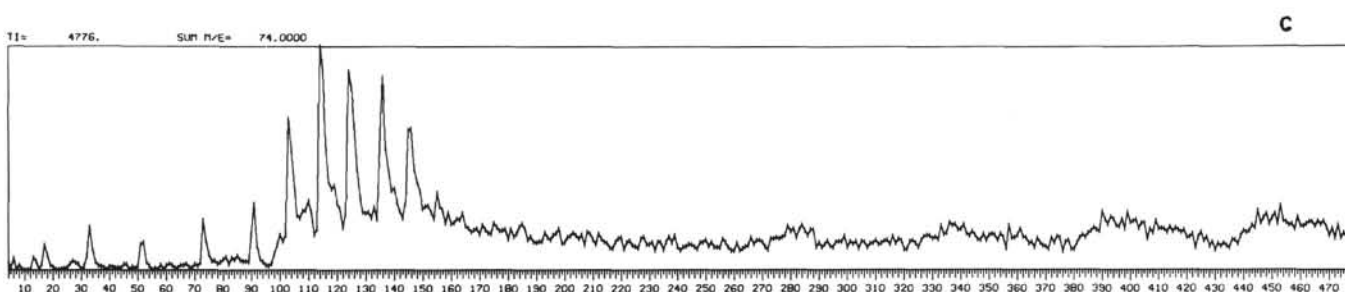
585

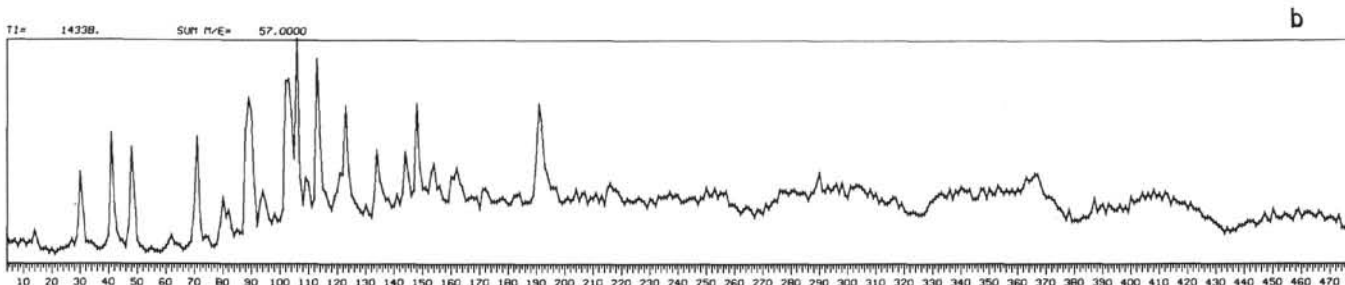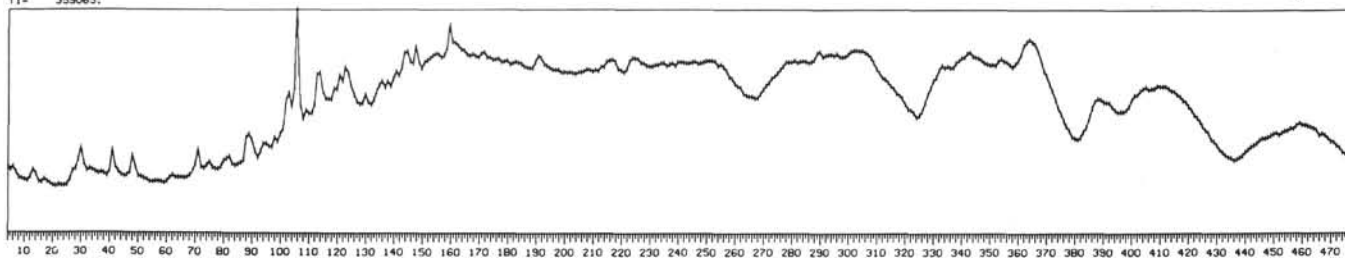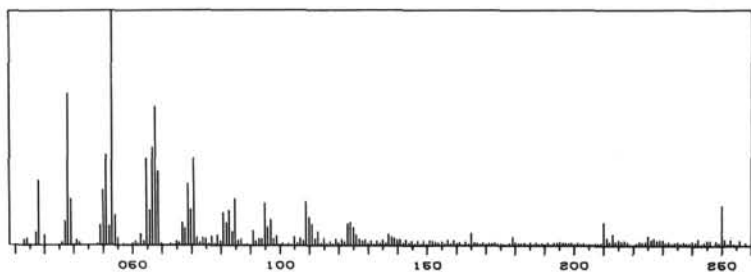B. R. SIMONEIT, E. S. SCOTT, A. L. BURLINGAME

Figure 5. *GC/MS data for the total heptane-soluble extract from Sample 14-138-6-3 (49-50 cm). (GC conditions as cited in Figure 1a).*

a) *total ionization sum plot.*

b) *m/e 57 sum plot.*

c) *m/e 74 sum plot.*

d) *m/e 191 sum plot.*

e) *m/e 231 sum plot.*

f) *mass spectrum scan 106 (unknown, M-250).*

g) *mass spectrum scan 291 (cholestanone).*
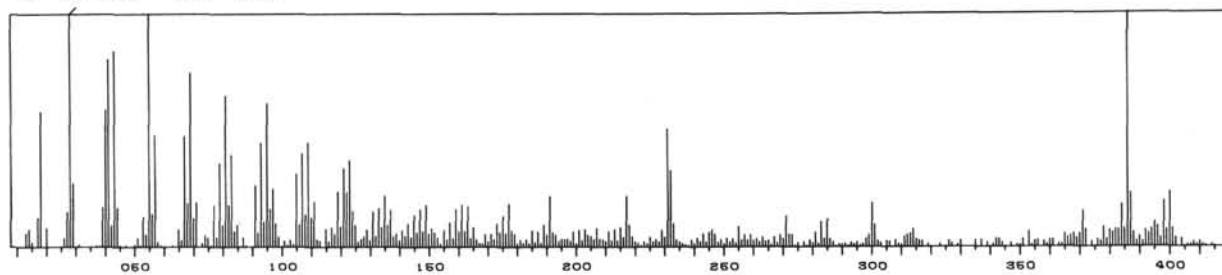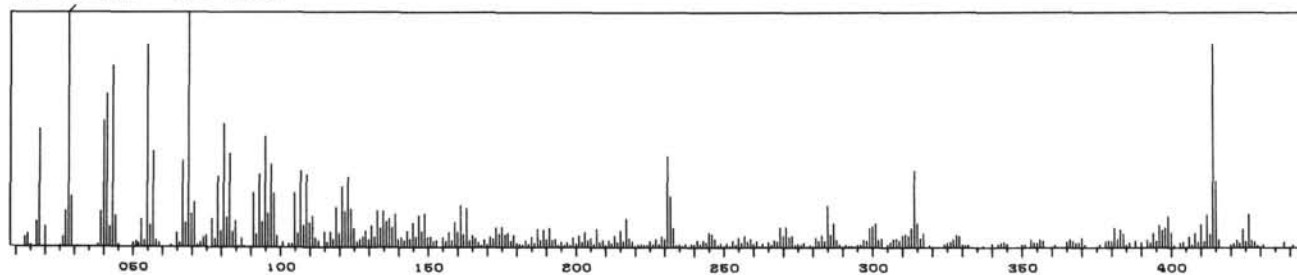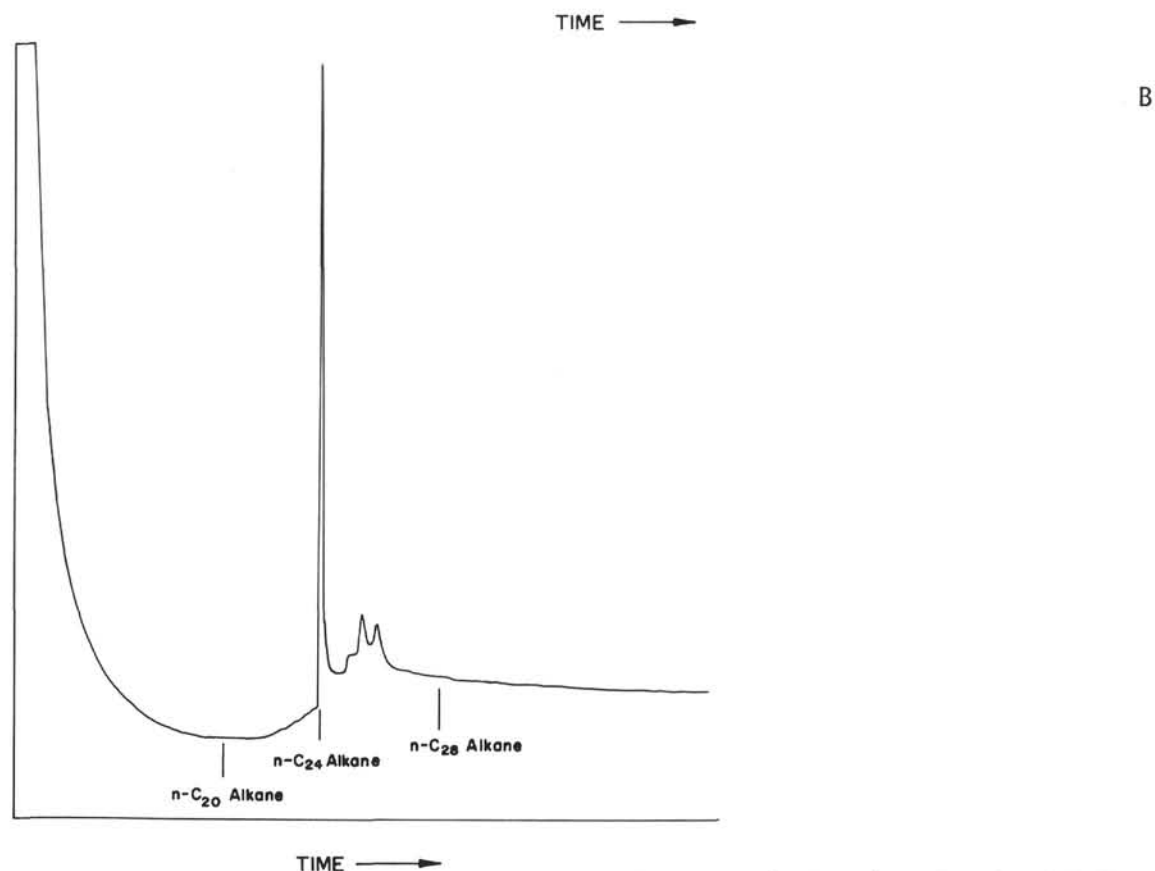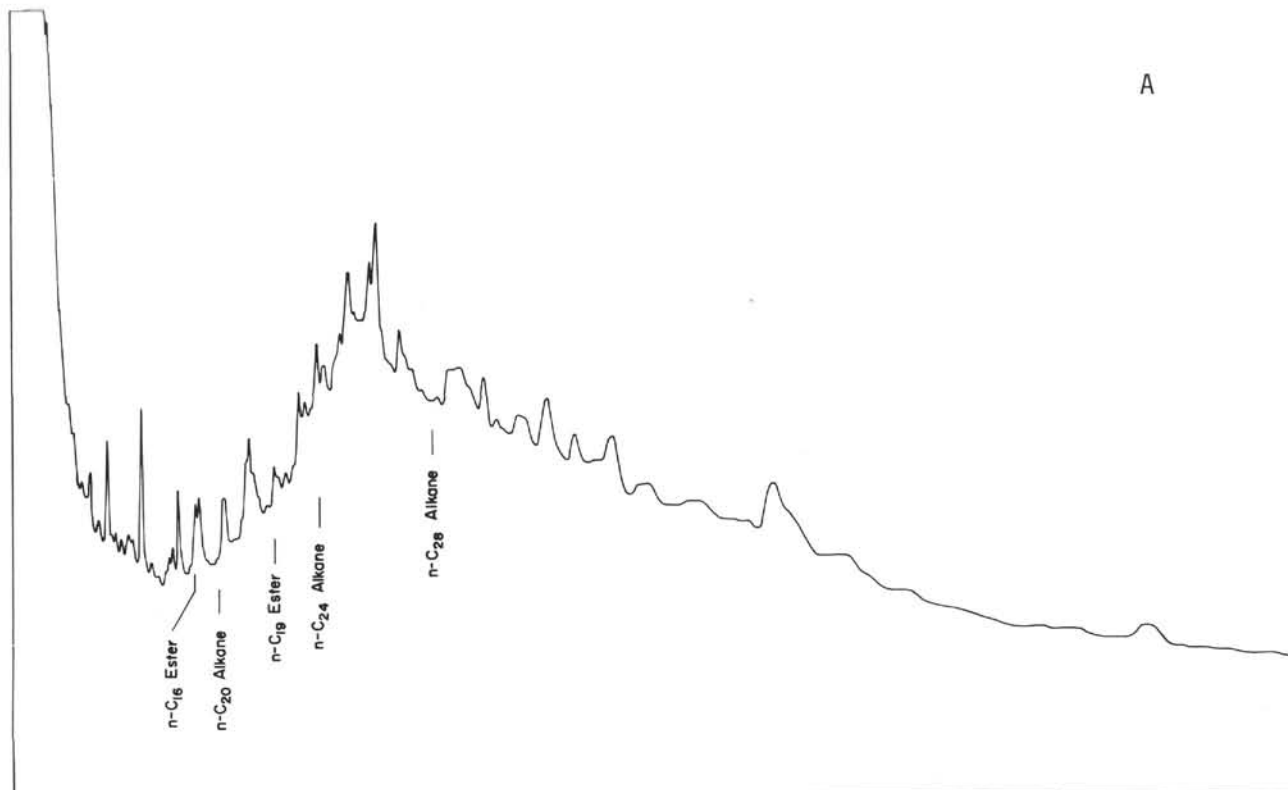
h) *mass spectrum scan 364 (stigmastanone).*

Figure 5. *(Continued)*.

Figure 6a. *Gas chromatogram of the heptane/ether-soluble extract fraction from Sample 14-144A-5-1 (114-116 cm). Conditions as cited in Figure 1a, except column length is 10 ft.*

Figure 6b. *Gas chromatogram of the benzene/methanol-soluble extract fraction from Sample 14-144A-5-1 (114-116 cm). Conditions as cited in Figure 4a.*

TABLE 4
Major Components of the Heptane-Ether Soluble Extracts from the Core Samples of
DSDP Site 144, Determined by GC/MS

Compound Name	Composition and Molecular Weight		Sample		
			14-144A-5-1 (114-116 cm)	14-144A-6-1 (100-101 cm)	14-144-4-3 (14-15 cm)
			Spectrum Scan No. (cf. Fig. 7a)	Spectrum Scan No. (cf. Fig. 9a)	Spectrum Scan No. (cf. Fig. 13a)
iso-Tetradecane	$C_{14}H_{30}$	198	n.d.	45	n.d.
Methyl n-undecanoate	$C_{12}H_{24}O_2$	200	n.d.	n.d.	49
Methyl laurate	$C_{13}H_{26}O_2$	214	n.d.	n.d.	66
Pentadecane	$C_{15}H_{32}$	212	49	n.d.	n.d.
Diethyl phthalate[b]	$C_{12}H_{14}O_4$	222	61	n.d.	75
Methyl n-tridecanoate	$C_{14}H_{28}O_2$	228	n.d.	n.d.	84
Hexadecane	$C_{16}H_{34}$	226	67	62	78
Pristane	$C_{19}H_{40}$	268	n.d.	n.d.	98
Heptadecane	$C_{17}H_{36}$	240	82	87	100
Methyl myristate	$C_{15}H_{30}O_2$	242	83	88	102
Unknown	–	266	n.d.	n.d.	108
n-Octadecane	$C_{18}H_{38}$	254	95	102	123
Methyl n-pentadecanoate	$C_{16}H_{32}O_2$	256	96	115	126
Unknown	–	250	99	120	n.d.
iso-Nonadecane	$C_{19}H_{40}$	268	n.d.	n.d.	141
Unknown	–	306	n.d.	128	n.d.
n-Nonadecane	$C_{19}H_{40}$	268	109	133	153
Methyl palmitate	$C_{17}H_{34}O_2$	270	110	135	157
Dibutyl phthalate[b]	$C_{16}H_{22}O_4$	278	112	n.d.	159
n-Eicosane	$C_{20}H_{42}$	282	127	153	173
Methyl margarate	$C_{18}H_{36}O_2$	284	128	154	175
Dibutyl azelate[a]	$C_{17}H_{32}O_4$	300	n.d.	159	181
Methyl stearate	$C_{19}H_{38}O_2$	298	143	172	188
Docosene	$C_{22}H_{44}$	308	n.d.	172	n.d.
n-Heneicosane	$C_{21}H_{44}$	296	147	171	187
Dibutyl sebacate[a]	$C_{18}H_{34}O_4$	314	n.d.	177	192
n-Docosane	$C_{22}H_{46}$	310	n.d.	186	200
Methyl nonadecanoate	$C_{20}H_{40}O_2$	312	157	188	201
Dibutyl hendecanedioate[a]	$C_{19}H_{36}O_4$	328	n.d.	192	n.d.
Methyl arachidate	$C_{21}H_{42}O_2$	326	171	201	217
n-Tetracosane	$C_{24}H_{50}$	338	n.d.	213	232
Methyl heneicosanoate	$C_{22}H_{44}O_2$	340	183	214	234
n-Pentacosane	$C_{25}H_{52}$	352	n.d.	227	252
Unknown	–	378	n.d.	228	n.d.
Unknown	–	444	191	228	n.d.
Methyl behenate	$C_{23}H_{46}O_2$	354	197	229	255
Hexacosane	$C_{26}H_{54}$	366	n.d.	245	277
Unknown	–	446	n.d.	246	n.d.
Methyl tricosanoate	$C_{24}H_{48}O_2$	368	n.d.	247	282
Heptacosane	$C_{27}H_{56}$	380	n.d.	264	297
Methyl lignocerate	$C_{25}H_{50}O_2$	382	n.d.	268	308
Unknown	–	460	n.d.	277	n.d.

<div style="text-align:center">TABLE 4 – Continued</div>

Compound Name	Composition and Molecular Weight		14-144A-5-1 (114-116 cm) Spectrum Scan No. (cf. Fig. 7a)	14-144A-6-1 (100-101 cm) Spectrum Scan No. (cf. Fig. 9a)	14-144-4-3 (14-15 cm) Spectrum Scan No. (cf. Fig. 13a)
Octacosane	$C_{28}H_{58}$	394	n.d.	283	318
Unknown	–	476	211	306	n.d.
Unknown	–	474	211	314	n.d.
Cholestane	$C_{27}H_{48}$	372	n.d.	314	320
Ergostane	$C_{28}H_{50}$	386	n.d.	n.d.	333
Sterane	$C_{28}H_{48}$	384	n.d.	n.d.	333
Triterpane	$C_{30}H_{48}$	408	225	n.d.	n.d.
Stigmastane	$C_{29}H_{52}$	400	225	n.d.	349
Triterpane	$C_{30}H_{54}O$	430	240	n.d.	n.d.
Unknown	–	490	n.d.	321	n.d.
Unknown	–	488	n.d.	336	n.d.

[a]Probably core tube contamination.

[b]Probably bagging contamination.

n.d. – Not detected.
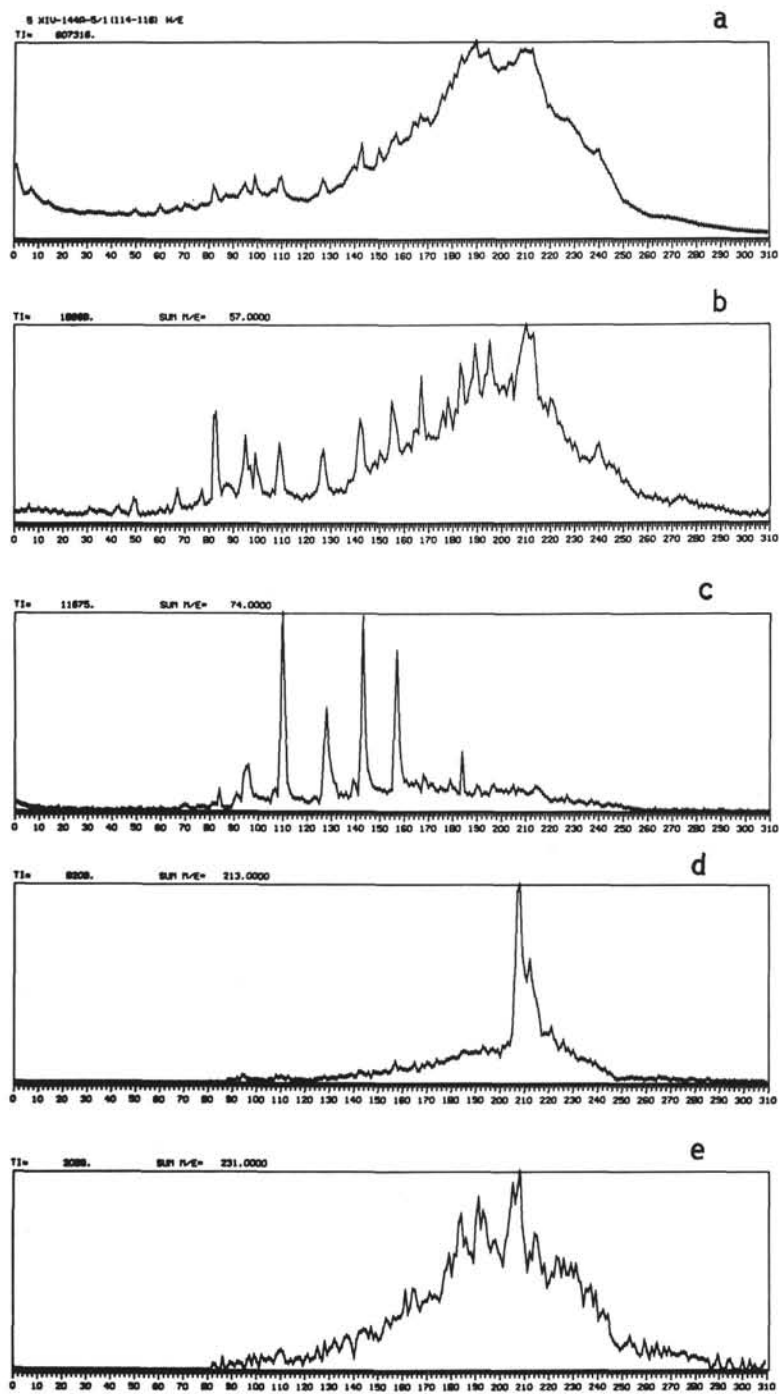
Figure 7. *GC/MS data for the total heptane-soluble extract from Sample 14-144A-5-1 (114-116 cm). (GC conditions as cited in Figure 1a).*

a) *total ionization sum plot.*

b) *m/e 57 sum plot.*

c) *m/e 74 sum plot.*

d) *m/e 213 sum plot.*
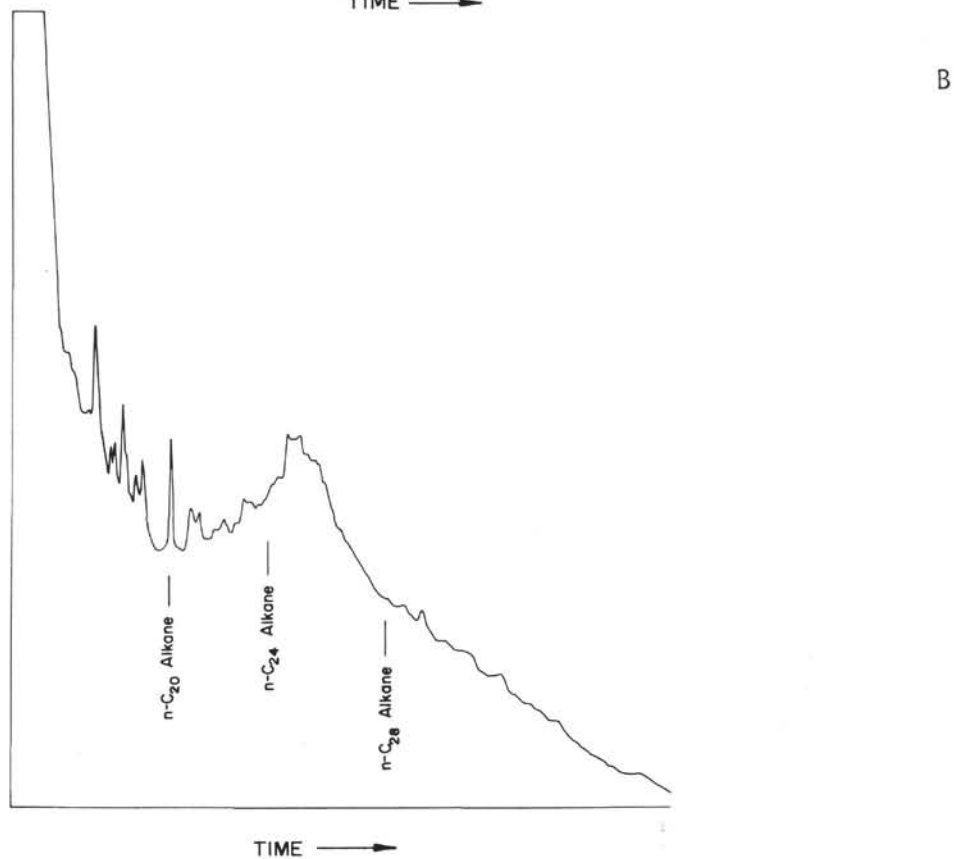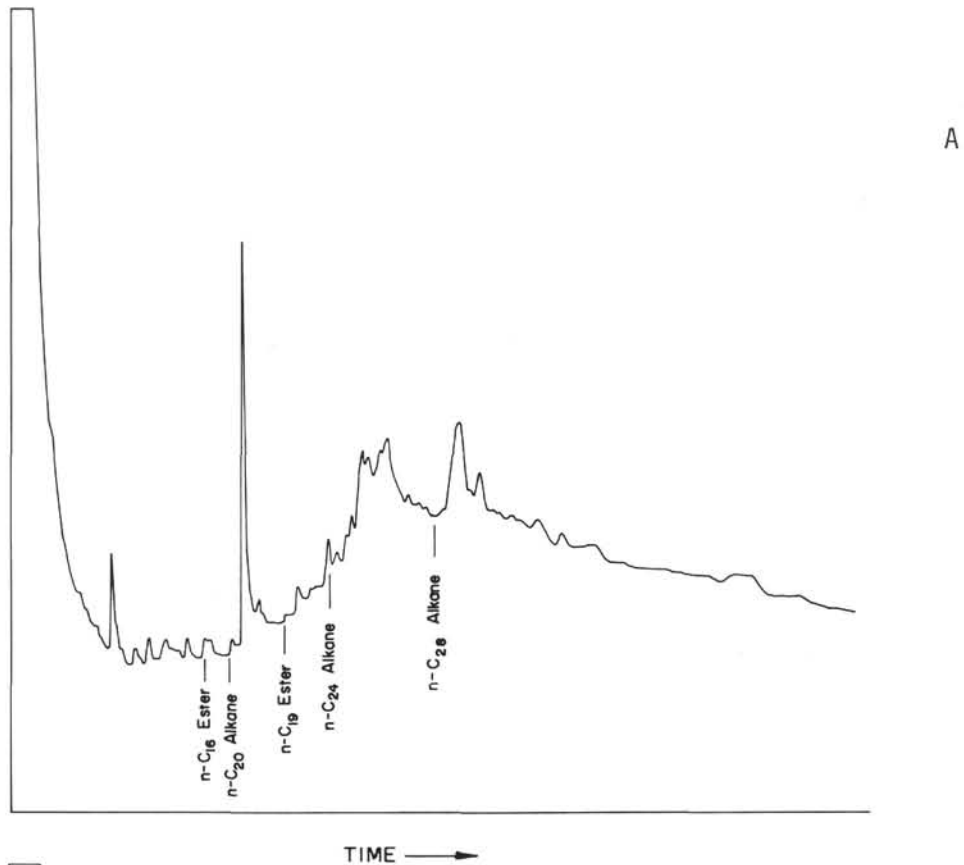
e) *m/e 231 sum plot.*

Figure 8a. *Gas chromatogram of the heptane/ether-soluble extract fraction from Sample 14-144A-6-1 (100-101 cm). Conditions as cited in Figure 4a.*
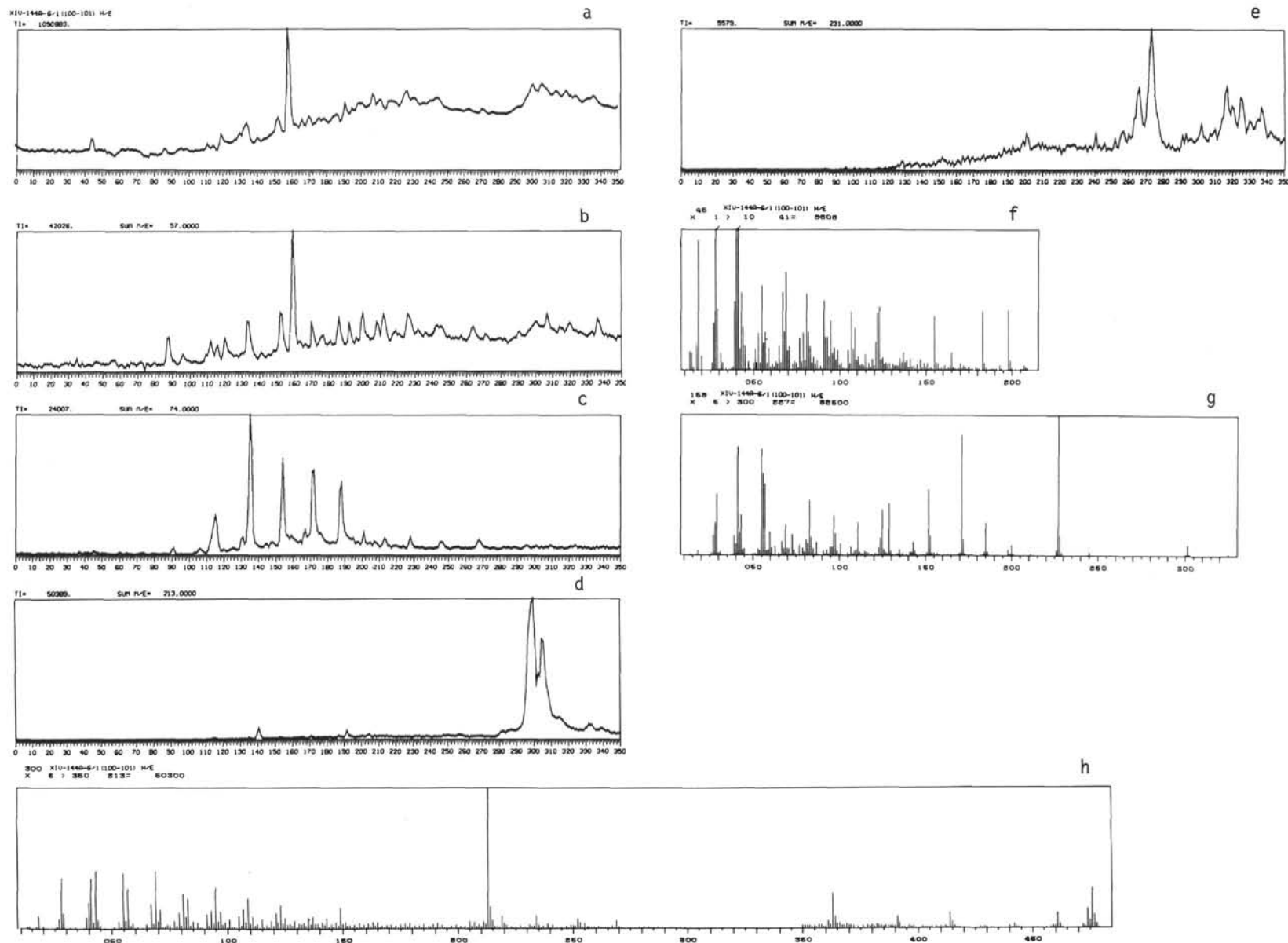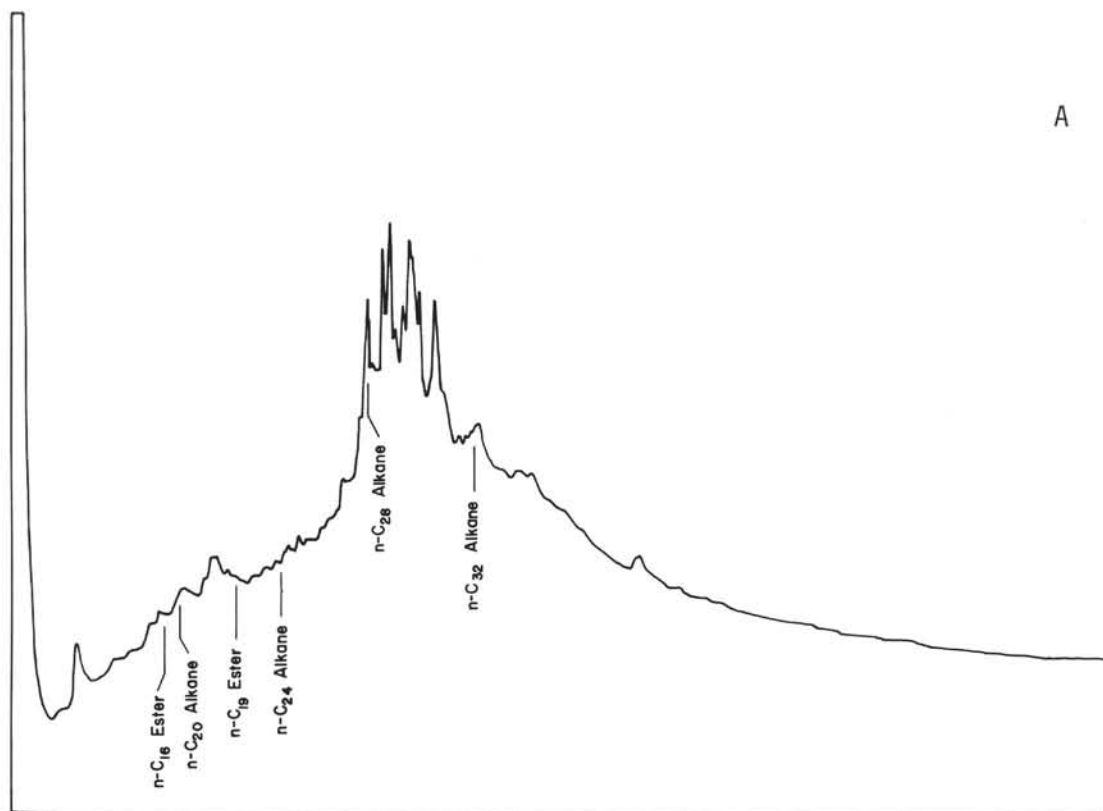
Figure 8b. *Gas chromatogram of the benzene/methanol-soluble extract fraction from Sample 14-144A-6-1 (100-101 cm). Conditions as cited in Figure 4a.*
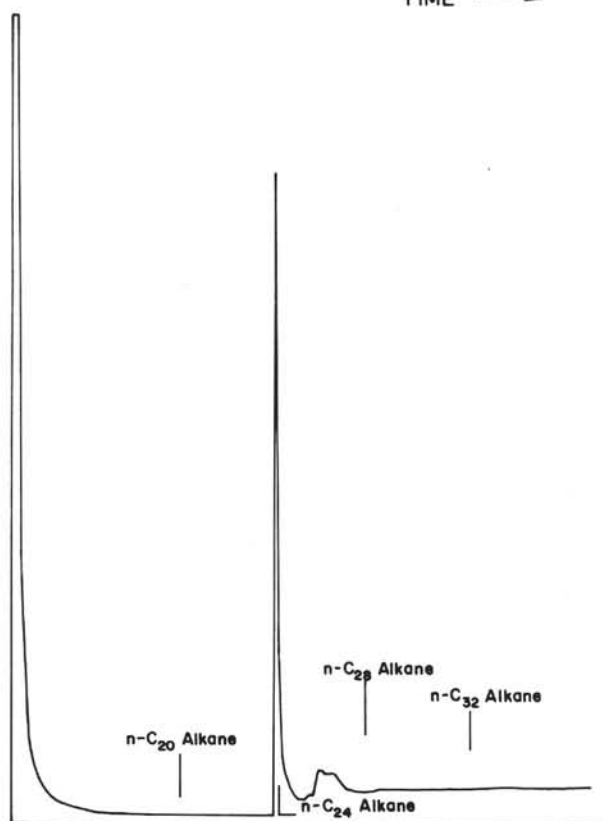
Figure 9. *GC/MS data for the total heptane-soluble extract from Sample 14-144A-6-1 (100-101 cm). (GC conditions as cited in Figure 1a).*

a) *total ionization sum plot.*   e) *m/e 231 sum plot.*
b) *m/e 57 sum plot.*   f) *mass spectrum scan 45 (iso-tetradecane).*
c) *m/e 74 sum plot.*   g) *mass spectrum scan 159 (dibutyl azelate).*
d) *m/e 213 sum plot.*   h) *mass spectrum scan 300 (unknown, M-576).*

Figure 10a. *Gas chromatogram of the heptane/ether-soluble extract fraction from Sample 14-144-4-2 (20-21 cm). Conditions as cited in Figure 1a.*

Figure 10b. *Gas chromatogram of the toluene/methanol-soluble extract fraction from Sample 14-144-4-2 (20-21 cm). Conditions as cited in Figure 1a.*
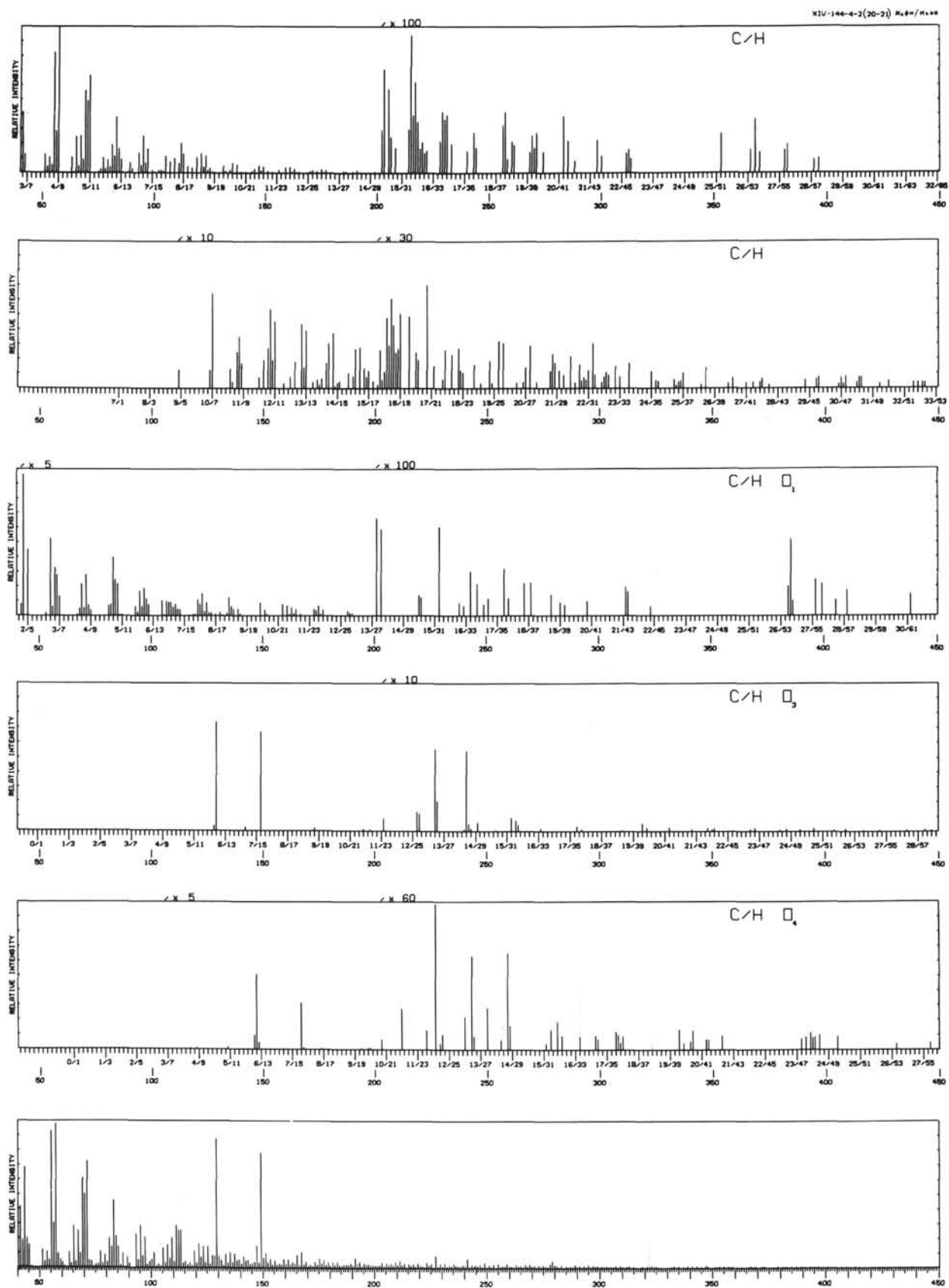
Figure 11. *Partial high resolution mass spectrometric data for the toluene- and methanol-soluble fraction from the exhaustive extract of Sample 14-144-4-2 (20-21 cm).*
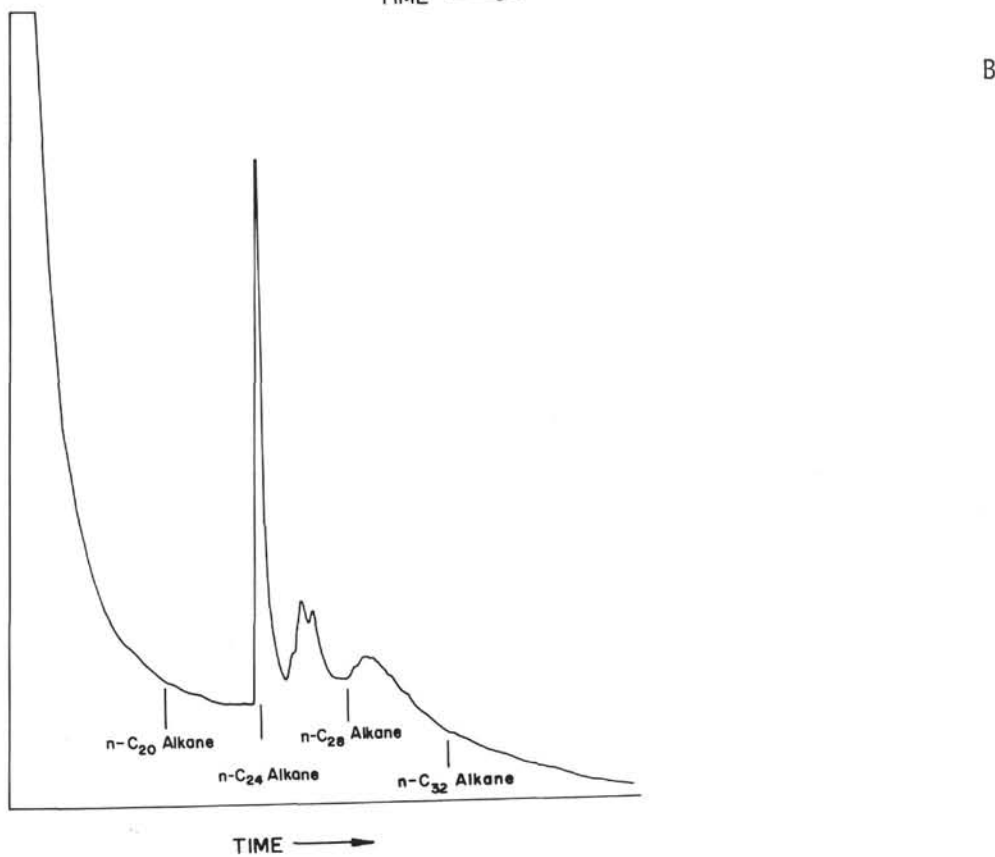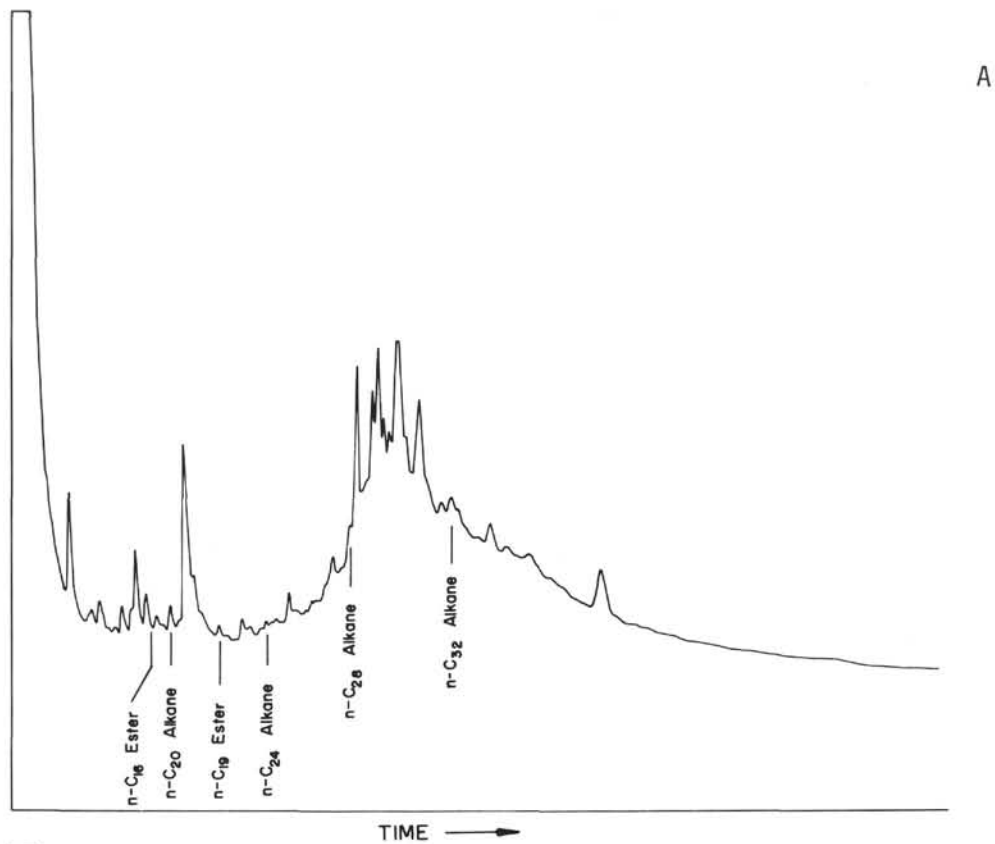
Figure 12a. *Gas chromatogram of the heptane/ether-soluble extract fraction from Sample 14-144-4-3 (14-15 cm). Conditions as cited in Figure 1a.*

Figure 12b. *Gas chromatogram of the benzene/methanol-soluble extract fraction from Sample 14-144-4-3 (14-15 cm). Conditions as cited in Figure 1a.*
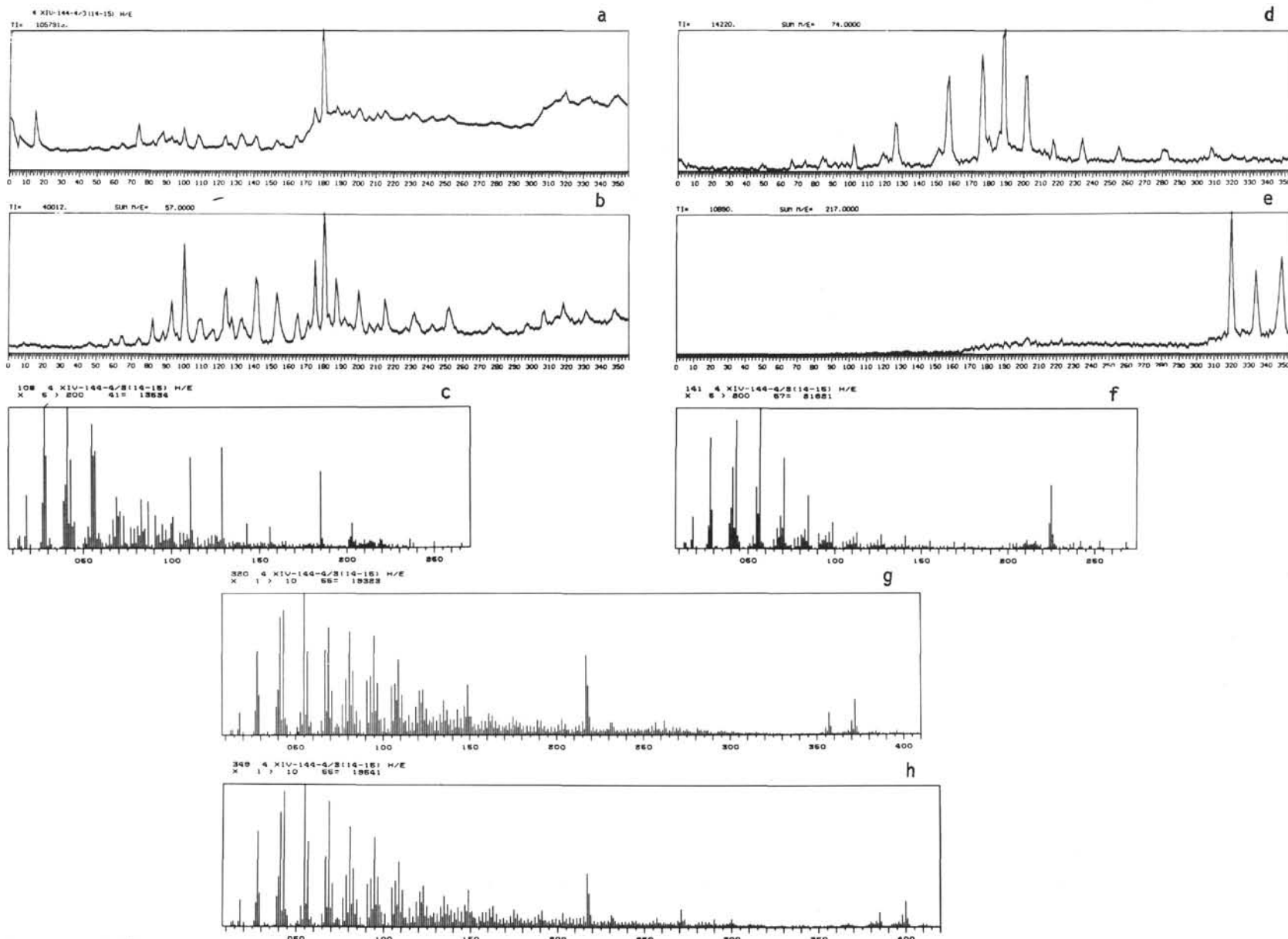
Figure 13. *GC/MS data for the total heptane-soluble extract from Sample 14-144-4-3 (14-15 cm). (GC conditions as cited in Figure 1a).*

a) *total ionization sum plot.*
b) *m/e 57 sum plot.*
c) *m/e 74 sum plot.*
d) *m/e 217 sum plot.*

e) *mass spectrum scan 108 (unknown, M-266).*
f) *mass spectrum scan 141 (iso-nonadecane).*
g) *mass spectrum scan 320 (cholestane).*
h) *mass spectrum scan 349 (stigmastane).*
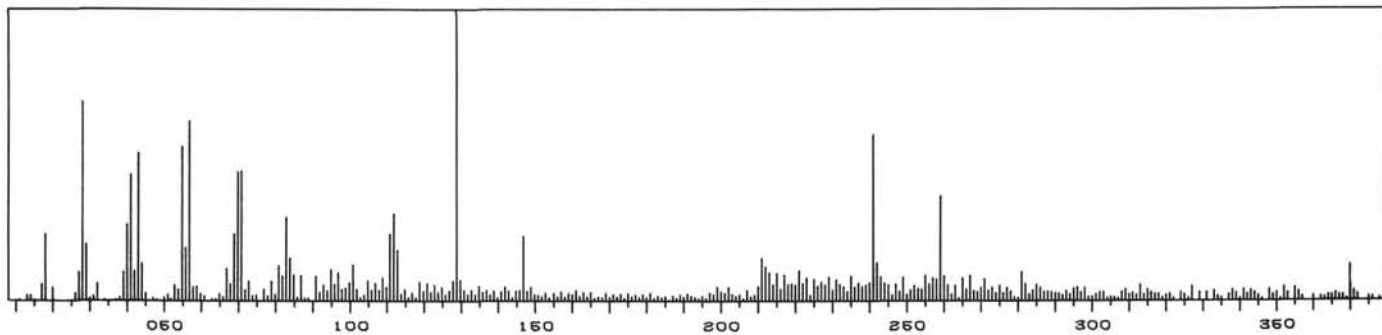
B. R. SIMONEIT, E. S. SCOTT, A. L. BURLINGAME

Figure 14. *GC/MS scan of the major peak in the benzene/methanol-soluble fraction from Sample 14-144-4-2 (20-21 cm) — scan 248 (probably dioctyl 2,3-dimethylsuccinate).*
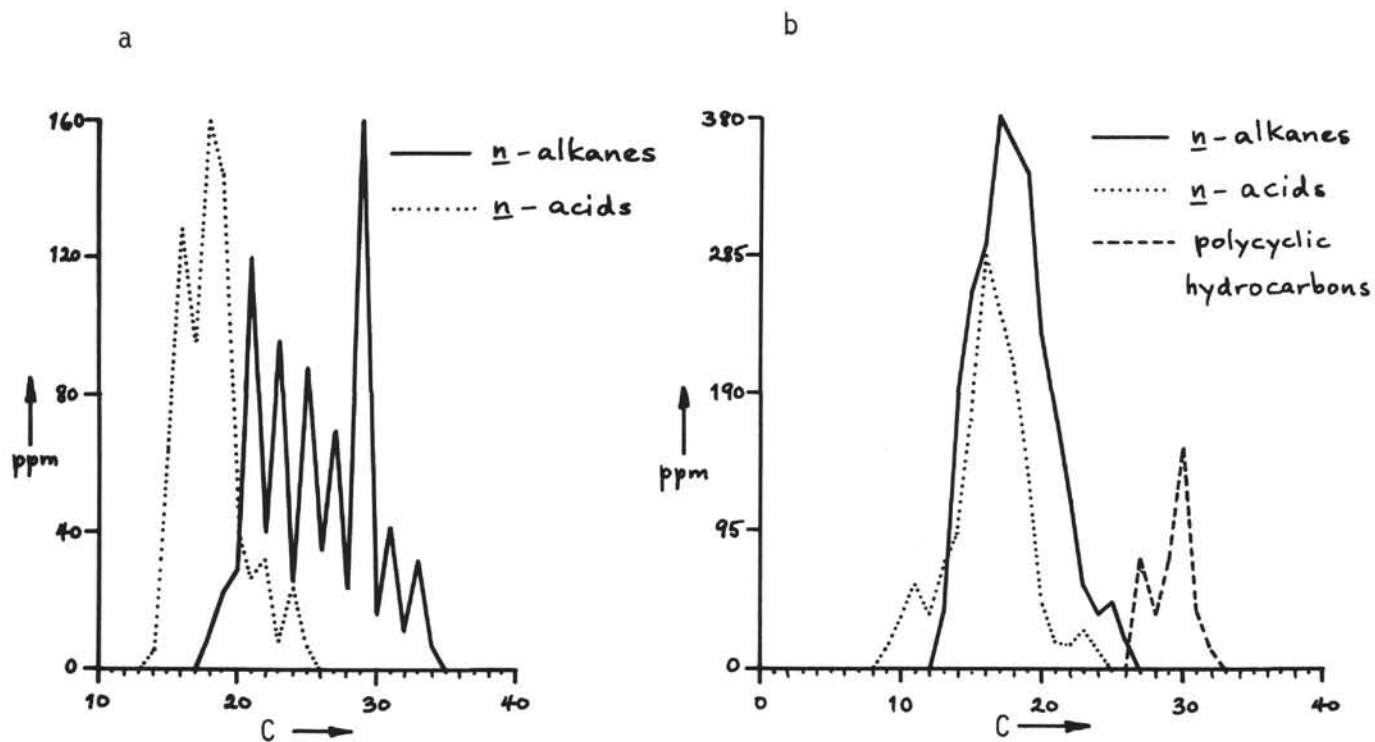

Figure 15. *Homologous series distribution histograms for the Site 138 samples.*
   a) *14-138-2-6 (12-13 cm).*
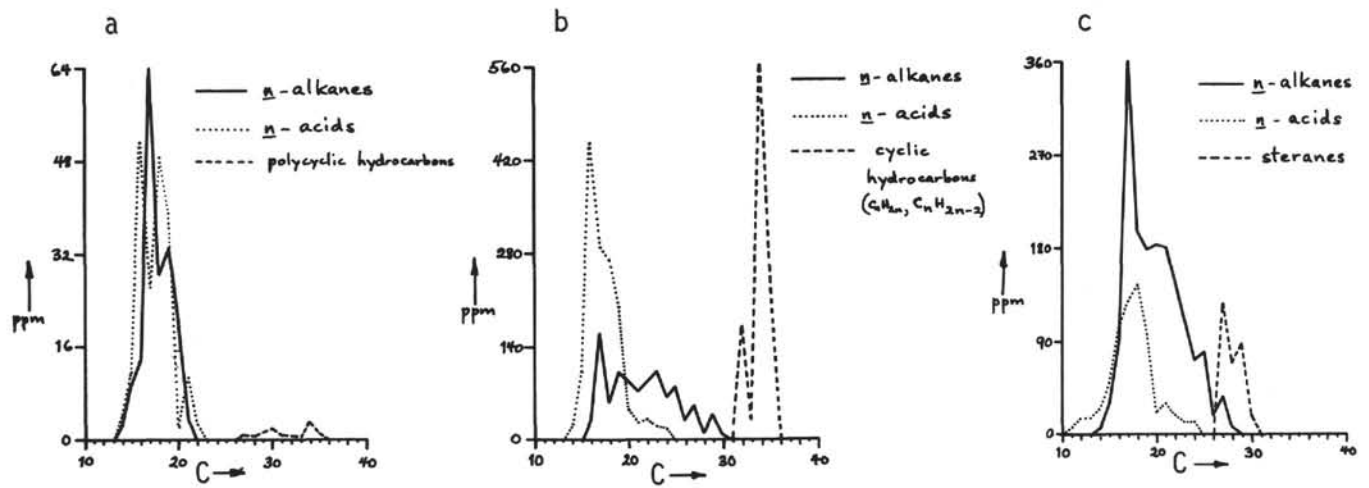   b) *14-138-6-3 (49-50 cm).*

Figure 16. *Homologous series distribution histograms for the Site 144 samples.*
  a) *14-144A-5-1 (114-116 cm).*
  b) *14-144A-6-1 (100-101 cm).*
  c) *14-144-4-3 (14-15 cm).*

Sample 14-144-4-3 (14-15 cm) contains mainly three homologous series: alkanes with no predominance and a maximum at C_{17}; acids with no predominance and a maximum at C_{18}; and steranes, consisting of cholestane ergostane, and sitostane (cf. Figure 16c). The narrow distribution envelope of the alkanes and acids and the sterane distribution indicate a marine source for the soluble organic matter.

The bulk of the organic matter in these Cretaceous samples consists of kerogen. The extractable petroliterous material appears to have derived from marine sources and has gone through diagenetic maturation.

ACKNOWLEDGMENTS

REFERENCES

Arpino, P. and Ourisson, G. 1971. Interactions between rock and organic matter. Esterification and transesterification induced in sediments by methanol and ethanol. Anal. Cham. **43**, 1656.

Budzikiewicz, H. and Djerassi, C., 1962. Mass spectrometry in structural and stereochemical problems. I. Steroid ketones. J. Am. Chem. Soc. **84**, 1430.

Burlingame, A. L., 1968. Data acquisition, processing and interpretation *via* coupled high-speed real-time digital computer and high resolution mass spectrometer systems. *In* Advances in Mass Spectrometry, Vol. 4, E. Kendrick (Ed.). London (The Institute of Petroleum). 15.

———, 1970. Developments and applications of real-time high resolution mass spectrometry. *In* Recent Developments in Mass Spectroscopy, K. Ogata and T. Hayakawa (Eds.). Tokyo (University of Tokyo Press). 104.

Burlingame, A. L. and Smith, D. H., 1968. Automated heteroatomic plotting as an aid to the presentation and interpretation of high resolution mass spectral data. Tetrahedron. **24**, 5749.

Burlingame, A. L., Smith, D. H., Merren, T. O. and Olsen, R. W., 1970. Real-time high resolution mass spectrometry. *In* Computers in Analytical Chemistry (Vol 4, Progress in Analytical Chemistry Series), C. H. Orr and J. Norris (Eds). New York (Plenum Press). 17

Chang, J. J., Walls, F. C., Smith, D. H., Simoneit, B. R. and Burlingame, A. L., in preparation. The LOGOS compound classifier for background corrected low resolution mass spectral data. Anal. Chem.

Hayes, D. E., Pimm, A. C., Benson, W. E., Berger, W. H., von Rad, U., Supko P. R., Beckmann, J. P., Roth, P. H. and Musich, L. F., 1971. Deep Sea Drilling Project Leg 14. Geotimes. **16**(2), 14.

Hayes, D. E., Pimm, A. C. et al., 1972. Initial Reports of the Deep Sea Drilling Project, Volume 14. Washington (U.S. Government Printing Office).

Maxwell, J. R., Douglas, A. G., Eglinton, G. and McCormick, A., 1968. The botryococcenes — hydrocarbons of novel structure from the alga *Botryoccoccus braunii*, Kützing. Phytochemistry. **7**, 2157.

Meyers, P. A. and Quinn, J. G., 1971. Fatty acid-clay mineral association in artificial and natural sea water solutions. Geochim. Cosmochim. Acta. **35**, 628.

Simoneit, B. R., in press. Organic analyses of the Black Sea cores. In the Black Sea: Geology, Chemistry and Biology, E. T. Degens and D. A. Ross (Eds.). Am. Assoc. Petrol. Geologists Mem.

Simoneit, B. R. and Burlingame, A. L., 1971a. Some preliminary results on the higher weight hydrocarbons and fatty acids in the Deep Sea Drilling Project cores, Legs 5-7. *In* Winterer, E. L., Riedel, W. R. et al., 1971. Initial Reports of the Deep Sea Drilling Project, Volume 7. Washington (U.S. Government Printing Office). 889.

———, 1971b. Further preliminary results on the higher weight hydrocarbons and fatty acids in the Deep Sea Drilling Project cores, Legs 5-8. *In* Tracey, J. I., Jr., Sutton, G. H. et al., 1971. Initial Reports of the Deep Sea Drilling Project, Volume 8. Washington (U. S. Government Printing Office). 8973.

———, 1972a. Further preliminary results on the higher weight hydrocarbons and fatty acids in the Deep Sea Drilling Project cores, Leg 9. *In* Hays, J. et al., 1972. Initial Reports of the Deep Sea Drilling Project, Volume 9. Washington (U.S. Government Printing Office). 859.

———, 1972b. Preliminary organic analyses of the Deep Sea Drilling Project (JOIDES) cores, legs V-IX. *In* Advances in Organic Geochemistry 1971, H. R. von Gaertner and H. Wehner (Eds.). Braunschwig (Pergamon-Vieweg). 189.

Simoneit, B. R., Scott, E. S., Howells, W. G. and Burlingame, A. L., 1972. Preliminary organic analyses of the Deep Sea Drilling Project cores from Leg 11. *In* Hollister, C. D., Ewing, J. I. et. al. 1972. Initial Reports of the Deep Sea Drilling Project, Volume 11. Washington (U.S. Government Printing Office). 1013.

Simoneit, B. R., Scott, E. S. and Burlingame, A. L., in press. Preliminary organic analyses of Deep Sea Drilling Project cores from Legs 12 and 13. *In* Ryan, W. B., Hsu, K. J. et al. Initial Reports of the Deep Sea Drilling Project, Volume 13. Washington (U.S. Government Printing Office).

———, in preparation. Preliminary organic analyses of the Deep Sea Drilling Project Cores, Leg 10. *In* Worzel, J. L., Bryant, W. et al. Initial Reports of the Deep Sea Drilling Project. Volume 10. Washington (U.S. Government Printing Office).

Simoneit, B. R., Howells, W. G. and Burlingame, A. L., in preparation. Preliminary organic geochemical analyses of the Cariaco Trench Site 147, Deep Sea Drilling Project, Leg 15. *In* Edgar, N. T., Saunders, J. B. et al. Initial Reports of the Deep Sea Drilling Project, Volume 15. Washington (U.S. Government Printing Office).

Smith, D. H., 1972. A compound classifier based on computer analysis of low resolution mass spectral data. Geochemical and environmental applications. Anal. Chem. **44**, 536.

Smith, D. H., Olsen, R. W., Walls, F. C. and Burlingame, A. L., 1971. Real-time organic mass spectrometry: LOGOS — a generalized laboratory system for high and low resolution, GC/MS and closed-loop applications. Anal. Chem. **43**, 1796.